KAUNAS UNIVERSITY OF TECHNOLOGY

MECHANICAL ENGINEERING AND DESIGN FACULTY

Karthikeyan Murugesan

STRENGTH ANALYSIS OF SANDWICH COMPOSITE STRUCTURE LAMINATED BY GLASS FIBER REINFORCED PLASTICS

Final project for Master degree

Supervisor
Assoc. Prof. Dr. Paulius Griškevičius

KAUNAS, 2015

KAUNAS UNIVERSITY OF TECHNOLOGY
MECHANICAL ENGINEERING AND DESIGN FACULTY

STRENGTH ANALYSIS OF SANDWICH COMPOSITE STRUCTURE LAMINATED BY GLASS FIBER REINFORCED PLASTICS

Final project for Master degree

Masters in Mechanical Engineering (621H30001)

Supervisor
Assoc. Prof. Dr. Paulius Griškevičius

Reviewer
Assoc. Prof. Dr. Kazimieras Juzėnas

Project made by
Karthikeyan Murugesan

KAUNAS, 2015

KAUNAS UNIVERSITY OF TECHNOLOGY

Mechanical Engineering and Design Faculty

Karthikeyan Murugesan

Masters in Mechanical Engineering and 621H30001

"Strength analysis of sandwich composite structure laminated by glass fiber reinforced plastics"

DECLARATION OF ACADEMIC HONESTY

2015 June 12
Kaunas

I confirm that a final project by me, **Karthikeyan Murugesan**, on the subject "Strength analysis of sandwich composite structure laminated by glass fiber reinforced plastics" is written completely by myself; all provided data and research results are correct and obtained honestly. None of the parts of this thesis have been plagiarized from any printed or Internet sources, all direct and indirect quotations from other resources are indicated in literature references. No monetary amounts not provided for by law have been paid to anyone for this thesis.

I understand that in case of a resurfaced fact of dishonesty penalties will be applied to me according to the procedure effective at Kaunas University of Technology.

(name and surname filled in by hand) *(signature)*

KAUNAS UNIVERSITY OF TECHNOLOGY
FACULTY OF MECHANICAL ENGINEERING AND DESIGN

Approved:
Head of Mechanical Engineering Department

(Signature, date)

Vytautas Grigas
(Name, Surname)

MASTER STUDIES FINAL PROJECT TASK ASSIGNMENT
MASTERS IN MECHANICAL ENGINERING

The final project of Master studies to gain the master qualification degree, is research or applied type project, for completion and defence of which 30 credits are assigned. The final project of the student must demonstrate the deepened and enlarged knowledge acquired in the main studies, also gained skills to formulate and solve an actual problem having limited and (or) contradictory information, independently conduct scientific or applied analysis and properly interpret data. By completing and defending the final project Master studies student must demonstrate the creativity, ability to apply fundamental knowledge, understanding of social and commercial environment, Legal Acts and financial possibilities, show the information search skills, ability to carry out the qualified analysis, use numerical methods, applied software, common information technologies and correct language, ability to formulate proper conclusions.

1. Title of the Project

Strength Analysis of Sandwich Composite Structure Laminated by Glass Fiber Reinforced Plastics

Approved by the Dean 2015 y. May m.11 d. Order No. ST17-F-11-2

2. Aim of the project

Develop and validate the finite element simulation models for stress analysis on the composite sandwich structures with recycled paper based honeycomb core and glass fiber reinforced polymer facesheets fabricated by filament winding process.

3. Structure of the project

Literature review of composite materials and sandwich structures properties and manufacturing processes and modelling of composites and review of failure criteria for laminated fiber glass composite structures, Results from the analytical experimental and simulation obtained, conclusion.

4. Requirements and conditions

General Requirement for Master Thesis by KTU regulations and requirements.

5. This task assignment is an integral part of the final project
6. Project submission deadline: 2015 June 1st.

Given to the student Karthikeyan Murugesan

Task Assignment received Karthikeyan Murugesan
(*Name, Surname of the Student*) (*Signature, date*)

Supervisor Assoc. Prof. Dr. Paulius Griškevičius
(*Position, Name, Surname*) (*Signature, date*)

Murugesan, Karthikeyan. Strength analysis of sandwich composite structure laminated by glass fiber reinforced plastics. *Masters in mechanical engineering* final project / supervisor Assoc. Prof. Dr. Paulius Griškevičius; Kaunas University of Technology, Mechanical engineering and design faculty, Mechanical engineering department.

Kaunas, 2015. 77 p.

SUMMARY

The growing demand for light weight structures result in increasing replacement of metal parts by composite structures. It makes up about 65 per cent of all the composites produced today and is used for boat hulls, tanks, surfboards, sporting goods, swimming pool linings, building panels and car bodies. The wide use of composite structure comes from the ultimate strength of the glass fibers, core and resin combination. In the sandwich composite structure normally the bending loads are carried by the force couple formed by the facesheets and the shear loads are carried by the lightweight core material. The critical properties of the sandwich structure depends upon the application of the structure.

The main theme of this project is to perform stress analysis on the composite sandwich structure laminated by glass fiber reinforced plastics. In this thesis work a constitutive model for the numerical prediction of strength of Sandwich Composite Structure material behavior under three point bending, tension test and compression test. A tension test of the facesheet allowed verification of the material model and failure criteria of GFRP. Three-point bending of the sandwich and the compression of cylinder tests allowed verifying of the sandwich structure model. Using experimentally obtained specific material properties, a numerical finite element model of a hollow cylindrical structure was designed and experimentally verified. The designing and simulation of the model has been done in LS-PREPOST Beta 4.2 and LS-DYNA v.971 R7.0.0. *The stress analysis on the composite sandwich structure has been performed and the comparison of the results shows a good co-relation between finite element and experimental results. This methodology can be applied for all types of composite sandwich structures to determine the strength of the structures.*

Keywords: Sandwich composite, Failure criteria, Compression, Designing, Simulation.

Murugesan, Karthikeyan. Sluoksniuotų stiklo pluošto kompozitinių konstrukcijų stiprumo tyrimai. *Mechanikos inžinerijos magistro* baigiamasis darbas / vadovas Assoc. Prof. Dr. Paulius Griškevičius; Kauno technologijos universitetas, Mechanikos inžinerijos ir dizaino fakultetas, Mechanikos inžinerijos katedra.

Kaunas, 2015. 77 p.

SANTRAUKA

Didėjanti lengvųjų konstrukcijų paklausa įtakoja vis dažnesnį metalinių konstrukcijų pakeitimą kompozitinėmis. Tai sudaro apie 65 procentų visų šiandien gaminamų kompozitų naudojamų laivų korpusų, cisternų, banglenčių, sporto prekių, baseinų, statybinių plokščių ir kėbulų gamybai. Platus kompozitų panaudojimas nulemiamas stiklo pluošto stiprumo, korio ir dervos derinio. Sluoksniuotų kompozitų atveju lenkimo apkrovas priima laminate veikiančių vidinių jėgų poros, o šlyties apkrovas korys. Kritinės sluoksniuoto kompozito savybės priklauso nuo konstrukcijos taikymo srities.

Pagrindinis šio darbo tikslas yra atlikti sluoksniuotos kompozitinės konstrukcijos laminuotos stiklo pluoštu stiprumo analizę. Tempimo, gniuždymo ir lenkimo bandymais nustatytos kompozitinių medžiagų komponentų ir iš jų pagamintų struktūrų mechaninės savybės. Atlikti eksperimentiniai tyrimai naudojant įvairias stiklo pluošto kompozitų armavimo schemas, kurių rezultatai panaudoti skaitinių ir analitinių modelių validavimui. Baigtinių elementų metodu sukurtas skaitinis modelis leidžiantis prognozuoti sluoksniuotos kompozitinės konstrukcijos stiprumą ir deformavimosi elgseną. Skaitinis modelis patikrintas naudojant sluoksniuoto kompozito cilindrinio vamzdžio skersinio gniuždymo bandymus. Baigtinių elementų modelių kūrimui ir skaičiavimui panaudotos LS-PREPOST Beta 4.2 ir LS-DYNA v.971 R7.0.0 programos. Stiprumo analizė atlikta panaudojant skirtingus stiprumo kriterijus, tolimesnei analizei pasirinktas geriausiai eksperiementinius rezultatus atitinkantis stirpumo kriterijus ir medžiagos modelio konstantos. Pasiūlyta metodologija gali būti taikoma įvairių sluoksniuotų kompozitinių konstrukcijų stiprumo skaičiavimams.

Raktiniai žodžiai: Sluoksniuotas kompozitas, stiprumo kriterijai, projektavimas, modeliavimas, baigtinių elementų analizė.

TABLE OF CONTENTS

LIST OF FIGURES

Figures **Page No**

LIST OF TABLES

Tables **Page No**

INTRODUCTION

The need for light weight structures will lead to increasing replacement of metal parts by sandwich composite structures. The glass fiber composite was first introduced in 1940s. It was commonly used and the first new developed at that time. The composites which are used today consists of about 65% used worldwide for applications such as tanks, boats, furniture's and vehicle components.

Due to the high strength of fiber glass, core and resin mixture it can be commonly used for all types of composite structure. To create a research methodology to determine the strength of composite sandwich structures and to determine their properties.

Objective: The main objective of this project is to perform stress analysis on the composite sandwich structures with recycled paper based honeycomb core and glass fiber reinforced polymer facesheets fabricated by filament winding process.

Tasks to be performed:

1. Determine the material properties of glass fiber lamina.
2. Create analytical model.
3. To perform tension, three point bending and compression tests were to be conducted on the composite sandwich specimens.
4. Create and validate finite element models for tension, three point bending and ring compression tests.
5. Compare the numerical and experimental results using ring compression test.

1. LITERATURE REVIEW

1.1 History

The development of fiber-reinforced plastic which is used commercially have been researched comprehensively in the 1930s, considerable research was undertaken by pioneers such as Norman de Bruyne it may be due to the interest to the aviation industry [21].

Mass production of glass strands was discovered in 1932. Owens-Illinois researchers accidentally directed a jet of compressed air at a stream of molten glass and produced fibers [21]. A suitable resin for combining the "fiberglass" with a plastic was developed in 1936 by du Pont. Peroxide curing systems were used after the first ancestor of modern polyester resins is Cyanamid's of 1942 [21].

Russia constructed a passenger boat of plastic materials in 1939, and the United States fuselage and wings of an aircraft Ray Greene of Owens Corning is attributed with making the first composite boat in 1937, but due to the brittle nature of the plastic used they did not proceed further at the time [21]. The first car to have a fiber-glass body was the 1946 Stout Scaraband their is only one model was built [21].

Glass fibers are the most commonly used in all industries, though carbon-fiber and carbon-fiber-aramid composites are widely found in the aerospace, automotive and sporting applications [21]. In 1943, Republic Aviation Corporation made a significant development in the tooling for GFRP components [21].

In the mid 20th century the global polymer production on the scale which is currently available begins, polymer production become economical due to the combined effect of low material and productions costs, new production technologies and new product categories. The industry finally matured in the late 1970s when world production of polymer exceeds that of steel [21].

1.2 Composite

The composite materials are made up of matrix or binder, and the reinforcement. These two materials play an efficient role. Matrix or binder surrounds and binds together a cluster of fibers or fragments of a reinforcement which is a much stronger material as shown in (Figure 1.1). As In the case of mud bricks, the two materials are the mud and the straw; in the case of concrete the materials are cement and the aggregate; in case of piece of wood, it is by the cellulose and the lignin [17].

Figure 1.1: Sandwich composite Structure [17]

The threads of glass in fiberglass are very strong under tension but they can be also brittle in some scenario where they will snap if they bent sharply. The reinforcement is provided by fine threads or fibers of glass in the case of fiberglass, often woven into a sort of cloth, and the matrix is a plastic [17]. This matrix not only holds the fibers together, but also protects them from damage; this is because they divide the stress among them. The matrix is softened by suitable solvents to allow repairs to be made as it is soft enough [17].

A thin sheet is very strong because any deformation of a sheet of fiberglass stretches some of the glass fibers necessarily, and they are able to resist that. It possesses major advantage as it is quite light [17]. New composites have been developed with very valuable properties in recent decades. The matrix, and the manufacturing process brings them together carefully choosing the reinforcement, and the properties can be tailored by engineers to meet specific requirements [17]. They can, for example, make the composite sheet very strong in one direction by aligning the fibers that way, but weaker in another direction where strength is not so important, selecting the properties such as resistance to heat, chemicals, and weathering by choosing an appropriate matrix material [17].

1.3 Materials for the Matrix

The plastics are the polymers which hold the reinforcement together and help to decide the physical properties of the fianl product [6]. For the matrix, many modern composites use thermosetting or thermosoftening plastics also called as called resins, The use of plastics in the matrix explains the name 'reinforced plastics' commonly given to composites [17].

When prepared thermosetting plastics are liquid but when they are heated it is harden and become rigid (ie, they cure), these materials do not become soft under high temperatures as the setting process is irreversible [17]. Even when exposed to extreme environments these plastics also resist wear and attack by chemicals making them very durable [17].

Thermosoftening plastics are hard especially at low temperatures but they are soften when they are heated. When compared with thermosetting plastics they are less commonly used and also have some advantages, like greater fracture toughness, long shelf life of the raw material, capacity for recycling and a cleaner, safer workplace due to organic solvents are not needed for the hardening process [17].

Figure 1.2: Glass Fiber Reinforced Polymer [17]

Fiber-reinforced polymers or FRPs which are shown in (Figure 1.2) includes carbon-fiber reinforced plastic or CFRP, and glass-reinforced plastic or GRP. There are numerous thermoset composites, but advanced systems usually incorporate aramid fiber and carbon fiber in an epoxy resin matrix [17]. If classified by matrix then there are thermoplastic composites, short fiber thermoplastics, long fiber thermoplastics or long fiber-reinforced thermoplastics [17].

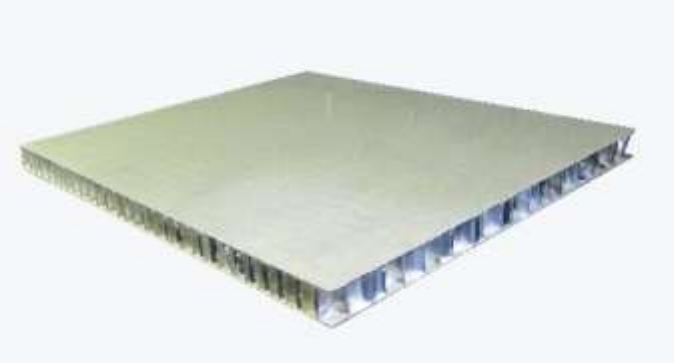

Figure 1.3: Sandwich Structured Composite [17]

A special class of composite material is fabricated by attaching two thin but stiff skins to a lightweight but thick core called the sandwich-structured composite (Figure 1.3). A low strength material is used as core material and its higher thickness provides the sandwich composite with low density overall high bending stiffness with [17].

1.4 Materials for the Reinforcement

The most common reinforcement used are the glass fibers but now advance composites with fine fibers of pure carbon are even used. Carbon fibers are much stronger and more expensive to produce. They are used in aircraft structures and in sporting goods and increasingly are used instead of metals to repair or replace damaged bones. Threads of boron are found to be stronger than carbon fibers [10].

1.5 The Manufacturing Process

The reinforcing material is first placed in the mould and then semi-liquid matrix material is pumped in generally to form the object. An object can be formed from a composite material by involving some form of mould usually. The mould is then heated to make the matrix set solid pressure may be applied to force out any air bubbles [5].

The molding process is often done by hand, but automatic processing by machines is becoming more common due to its high accuracy and relaiability. Pultrusion is nothing but a term derived from the words 'pull' and 'extrusion', which is one of the new method which is ideal for manufacturing products with high efficiency and these products should be straight which possess constant cross section [5].

By applying sheets of woven fiber reinforcement many thin structures with complex shapes (curved panels) with the composite structure is built up, saturated with the plastic matrix material, over an

appropriately shaped base mould [5]. The matrix material is then cured when the panel has been built to an appropriate thickness [5].

1.6 Processing of Fiber-Reinforced Composites

Processing of Fiber-Reinforced Composites is one of the major important aspect to be noted. To fabricate continuous fiber-reinforced plastics, the fibers should be uniformly distributed within the plastic matrix meeting with design specifications and in most cases everything is oriented in virtually the same direction [19]. Different techniques such as pultrusion, filament winding, and prepreg production processes by which useful products of these materials are manufactured will be discussed [25].

1.6.1 Pultrusion

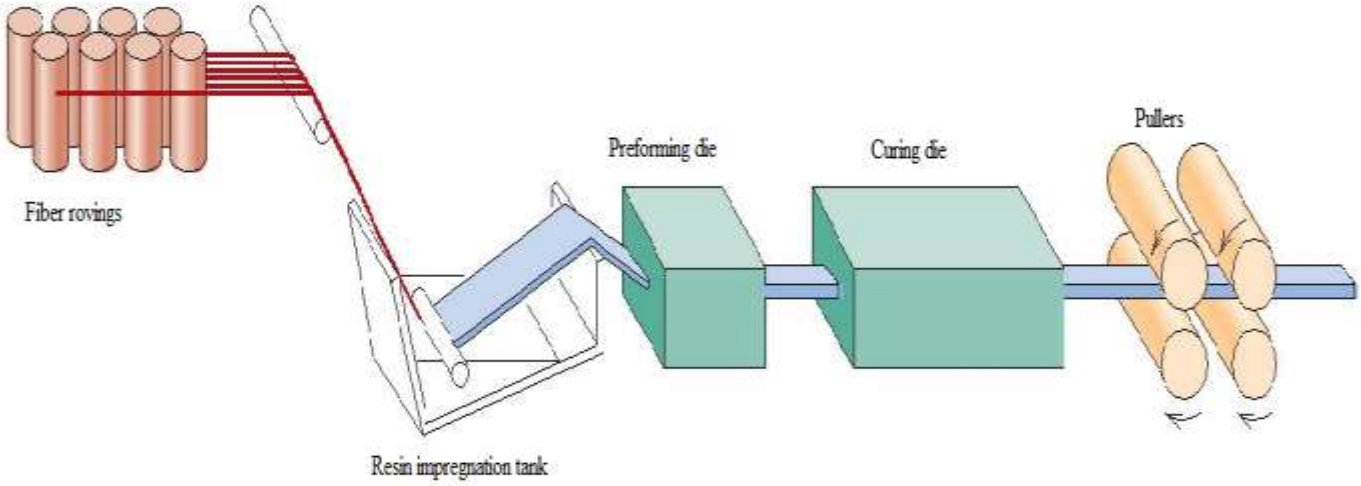

Figure 1.4: Schematic diagram showing the pultrusion process [25]

Pultrusion technique is illustrated schematically in (Figure 1.4), Pultrusion is used for the manufacture of components having continuous lengths and a constant cross-sectional shape (i.e., rods, tubes, beams, etc.) [25]. Continuous fiber rovings, or tows, 3 are first impregnated with a thermosetting resin; these are then pulled through a steel die that preforms to the desired shape and also establishes the resin/fiber ratio with the stock then passes through a curing die that is precision machined so as to impart the final shape; this die is also heated to initiate curing of the resin matrix [19]. A pulling device determines the production speed and also draws the stock through the dies and using center mandrels or inserted hollow cores tubes and hollow sections are made possible by using Principal reinforcements are glass, carbon, and aramid fibers, normally added in concentrations between 40 and 70 vol% [25].

Polyesters, vinyl esters, and epoxy resins are commonly used matrix materials. Pultrusion is a continuous process that is easily automated; production rates are relatively high, making it very cost effective and a wide variety of shapes are possible, and the length of stock that may be manufactured without any practical limit [25].

1.6.2 Prepreg Production Processes

Prepreg is a widely used composite industry's term which is used for continuous fiber reinforcement preimpregnated associated with a polymer resin that is only partially cured [25]. (Figure 1.5) The manufacturer received this material in tape form and later manufacturer directly molds and fully cures the product without having to add any resin which is probably the composite material form most widely used for structural applications [25].

The release paper sheet has been coated with a thin film of heated resin solution of relatively low viscosity so as to provide for its thorough impregnation of the fibers. A "doctor blade" spreads the resin into a film of uniform thickness and width [25]. The prepreging process begins by collimating a series of spool-wound continuous fiber tows that are then sandwiched and pressed using heated rollers between sheets of carrier paper, this process is termed as "calendering" [25]. The final prepreg product—the thin tape consisting of continuous and aligned fibers embedded in a partially cured resin which are prepared for packaging by winding onto a cardboard core [25].

The thermoset matrix undergoes curing reactions at room temperature ((the time in use at room temperature must be minimized)); therefore, the prepreg is stored lower. Both thermoplastic and thermosetting resins are utilized; carbon, glass, and aramid fibers are the common reinforcements [25]. Thermoset prepregs have a lifetime of at least six months and usually longer. Number of plies is laid up to provide the desired thickness after the effective removal from the carrier backing paper [25].

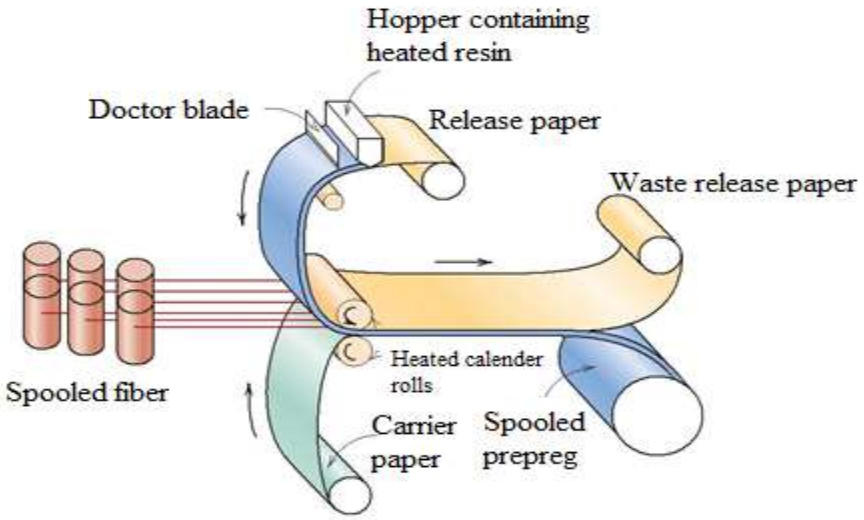

Figure 1.5: The production of prepreg tape using a thermoset polymer [25]

The lay-up arrangement procedure may be carried out entirely by hand (hand lay-up) and this lay-up may be unidirectional, usually the orientation of fiber is alternated to produce an angle-ply laminate [19]. Fabrication costs can be further reduced by automation of prepreg lay-up and other manufacturing procedures such as filament winding as shown in Figure 1.6, eliminating the need for hand labor. These automated methods are essential for many applications of composite materials to be cost effective, final curing is done by the instantaneous application of heat and pressure [25].

1.6.3 Filament Winding

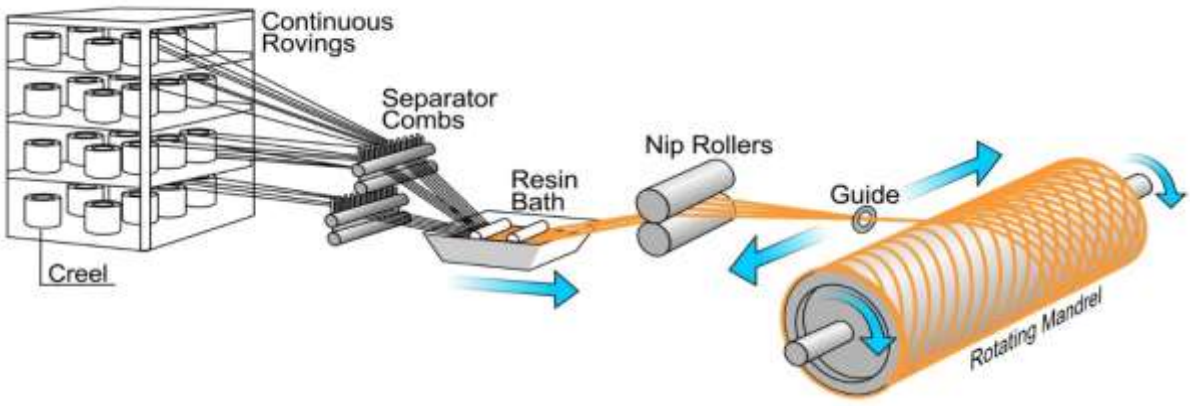

Figure 1.6: Filament winding process [19]

The process by which continuous reinforcing fibers are precisely located in a programmed pattern to form a cylindrical shape is termed as filament winding which is shown in (Figure 1.6) [19]. By using automated winding equipment the fibers are first fed through a resin bath either as individual strands or as tows and then are continuously wound onto a mandrel [19]. Curing is carried out at room temperature after the appropriate number of layers has been applied and later the mandrel is removed. To ensure the desired mechanical characteristics various winding patterns are possible such as circumferential, helical, and polar winding patterns. Rocket motor casings, storage tanks and pipes, and pressure vessels are most important filament-wound structures [19]. This technology is advancing very rapidly because it is very cost effective and filament-wound parts have a high degree of control over winding uniformity with very high strength-to-weight ratios and economically attractive when automated [19].

1.7 Constituents

1.7.1. Resins

Polymer-based composite materials, including fiberglass, carbon fiber, and Kevlar, include at least two parts, the substrate and the resin [17]. Polyester resin tend to have yellowish tint is suitable for most backyard projects as it is often used in the making of surfboards and in marine applications. When the peroxide is mixed with the resin, it decomposes to generate free radicals, which initiate the curing reaction [17]. Hardeners in these systems are commonly called catalysts, but since they do not re-appear unchanged at the end of the reaction, they do not fit the strictest chemical definition of a catalyst [17].

Vinyl ester resin having lower viscosity than polyester resin tends to have a purplish to bluish to greenish tint which possess more transparency and often billed as being fuel resistant, but will melt when it is in contact with gasoline [17]. Vinyl ester resin is highly flexible and tends to be more resistant over time to degradation than polyester resin. It uses the same hardeners as polyester resin (at a similar mix ratio) and the cost is approximately the same [17].

Epoxy resin is almost totally transparent when cured which is used as a structural matrix material or as structural glue and it possess a wide range of application in the aerospace industry [17].

Shape memory polymer (SMP) resins possess different visual characteristics depending on their formulation and they are epoxy-based, which is widely used for auto body and outdoor equipment repairs. These resins are unique as by heating above their glass transition temperature (T_g) their shape can be repeatedly changed, they become flexible and elastic when heated and they will maintain their new shape

Once they are cooled [17]. The advantage of shape memory polymer resins is that they can be shaped and reshaped repeatedly without losing their material properties and because of this phenomenon they can be effectively used in fabricating shape memory composites [17].

1.8 Reinforcement

1.8.1 Fiber

Figure 1.7: Differences in the way of fibers used for various applications [17]

Reinforcement possesses greater rigidity and impedes high crack propagation. Thin fibers can have very high strength, and provided they are mechanically well attached to the matrix they can greatly improve the composite's overall properties [17].

Fiber-reinforced composite materials (Figure 1.7) are divided into two major groups normally referred to as short fiber-reinforced materials and continuous fiber-reinforced materials [17]. The woven and continuous fiber styles (they often constitute a layered or laminated structure) are typically available in a variety of forms, being pre-impregnated with the given matrix (resin), dry, uni-directional tapes of various widths, plain weave, harness satins, braided, and stitched [17].

The short and long fibers are typically employed in compression moulding and sheet moulding operations as they come in the form of flakes, chips, and random mate [17]. Common fibers used for reinforcement include glass fibers, carbon fibers, cellulose and high strength polymers [17].

1.8.2 Influence of Fiber Strength

1.8.2.1 The Fiber Phase

The potential for reinforcement efficiency is greatest when compared with several composite types for those that are fiber reinforced. Significant reinforcement is possible only if the matrix-fiber bond is

strong [30]. An applied load is transmitted to and distributed among the fibers via the matrix phase with these composites, at least moderately ductile in most of the cases and in general fiber reinforcements are classified as whiskers, fibers, or wires bases on their diameter [30]. Reinforcement efficiency depends on fiber length as reinforcement discontinues at the fiber extremities. The length of continuous fibers greatly exceeds this critical value and the shorter fibers are discontinuous [30].

1.8.3 Influence of Fiber Orientation and Concentration

Fiber arrangement is also crucial relative to composite characteristics, for short and discontinuous fibrous composites, the fibers may be either aligned or randomly oriented. The mechanical properties of continuous and aligned fiber composites are highly anisotropic. In the alignment direction, reinforcement and strength are a maximum; perpendicular to the alignment, they are a minimum [19]. Significant strengths and stiffnesses are possible for aligned short-fiber composites in the longitudinal direction. Despite some limitations on reinforcement efficiency, the properties of randomly oriented short-fiber composites are isotropic [19].

1.8.4 Increase the Strength of Glass Fibers

The mechanical strength of pristine glasses is extremely high but the strength of practical glass products is much lower primarily due to surface flaws. However, these glasses can be made mechanically stronger by forming a compressive residual stress on the surface. There are two popular methods to produce a compressive surface stress on the glass surface: One is thermal tempering in which a glass product is heated to near the softening temperature and then rapidly cooled [20].

This produces a temperature gradient with the surface of the product being cooler than the interior, and at room temperature, a residual compressive stress results on the surface. Automotive side and rear windows are made stronger by this method. The second method is ion-exchange or chemical tempering, in which glasses containing smaller alkali ions, e.g. Na+, are treated in a molten salt containing larger alkali ions, e.g. K+, at a temperature below the glass transition temperature [21].

This process, sometimes called ion-stuffing, can produce a surface layer with an extremely high compressive stress on the glass and is currently employed to strengthen products such as aircraft windows and scratch resistant touch-screens on electronic devices. Although these processes are extremely effective in making glasses mechanically stronger, there are limitations to both. Tempering requires the product to

be of finite thickness, a few mm, in order to achieve the necessary temperature gradient during cooling. Ion-exchange processing requires the presence of alkali ions as a main glass component. In the present research, silica glass optical fibers were made stronger by an alternative compressive surface residual stress formation method [22]. The method is based upon a surface stress relaxation process while a sub-critical (i.e. a value less than the fracture strength) tensile stress is applied at a temperature, below the glass transition temperature, in the presence of water vapor, where upon release of the tensile stress a surface compressive stress is formed [22]. This mechanism was proposed previously, and the extent of surface residual stress formation was evaluated using a fiber bending method. Unlike alternative strengthening mechanisms, there is no minimum thickness or compositional requirement for its utilization. In the present paper the strengthening data of silica glass fibers treated at various temperatures in low water vapor pressure under various tensile stresses are presented together with the estimated surface residual compressive stress of fibers treated at various temperatures in the same atmosphere [22].

Silica glass fibers are known to become mechanically weaker when heat-treated at a temperature lower than the glass transition temperature in the presence of water vapor. However, the strength of silica fiber was found to become greater than the intrinsic fiber strength, when fibers were subjected to a sub-critical tensile stress during heat treatment [22]. The observed strengthening was attributed to surface compressive residual stress formation through surface stress relaxation during the sub-critical tensile stress application in the atmosphere containing water vapor [22]. Surface stress relaxation and surface residual stress formation of silica glass fibers were shown to take place under conditions similar to those experienced by the strengthened mechanical test specimens by observing permanent bending of the fiber. Furthermore, the presence of the surface residual compressive stress on uniaxially stressed and heated fibers was confirmed by observing the bending of the silica glass fibers upon slicing [22]. It was demonstrated that silica glass fibers can be strengthened to the value beyond the intrinsic strength by heat-treatment at a temperature far lower than the glass transition temperature in low water vapor pressure of ~6 Torr while the fiber is subjected to sub-critical tensile stress [22]. By this method it was possible to achieve an estimated failure stress of approximately 7–8 GPa for pure silica fiber in ambient atmospheric conditions, in contrast to a typical value of ~5.5 GPa. This process is proposed as an entirely new glass strengthening method which does not require glass of a minimum thickness, as in tempering, or a glass containing alkali ions, as in ion-exchange [23].

The search for new ways to improve the strength of glass has always been a hot topic, and E-glass is a composition of particular interest. E-glass is an alumino-borosilicate glass with a low alkali content

(b1 wt.%), that is employed where high strength and high electrical resistivity are desired. It is also the most widely used glass fiber in glass fiber-reinforced plastic (GFRP) composite applications. The market for E-glass fiber has expanded in recent years as GFRP composites see widespread usage in many industries as strong but lightweight materials [24].

1.8.5 Crack Growth in Glass Composites

The first physical effects of the environment on the glass/ polyester composites is liquid and gas absorption followed by swelling which occurs at a considerable rate. By increasing of swelling, growing internal stresses in the composite can cause fiber/matrix debonding [30].

Polyester resins contain considerable amount of some components which are soluble in water. After resolution, these substances produce osmotic pressure which cause micro cracks like disc-shaped cracks in resin [30].

Leaching and weight loss of matrix resin materials lead to shrinkage. Since all of these factors were strongly related to diffusion, it can clearly be said that environmental effect on composite was controlled by diffusion [30].

Stress corrosion crack growth on the glass or polyester composites can arise far below the fracture strength because glass fibers under stress are extremely sensitive to diluted acidic environment [28].

1.8.6 Creep of Polymer Composites

Actually glass fibers are well-known to suffer stress-rupture behavior under static loading conditions when exposed to moisture, also other agents, mainly acids. Creep considerably affected life, but was a less than order of magnitude effect, at least at room temperature. The creep will play a much more important role when at elevated temperature. Both diffusion & corrosion rate would also be considerably affected by temperature [29].

1.9 Cores

1.9.1 Paper Honey Comb

It is an evolutionary product that replaces non eco-friendly materials like (paper, wood, PUF, Rock Wool Mineral wool, EPS) in their respective applications while preserving the key virtues of their usage in the concerned applications. Paper Honey comb is an eco-friendly, adaptable, flexible and lightweight

material that has excellent similarity with other materials, in addition to it has excellent strength-to-weight ratio. Paper honey comb combines with steel, plywood, plastics, FRP and other materials while its sandwich faces to form some of the strongest composite panels for its weight and dimensions. It is cost-effective than other materials [11].

Since the product made from wastage paper (recycled paper) and eco-friendly glue, it is an advantage to the earth because of 100% bio-degradable, nonpolluting & eco-friendly material [11]. At present large usage of this honey comb can significantly increase a country's plan of preserving the nature. And it has many good properties when it compares with other similar materials, those properties are [11]:

- up to 95% open space [11]
- a density of 54 kg/m^3 (3.34 lb/ft^3) [11]

When bonded to a facing material on both the sides, the resulting sandwich panel offers the highest rigidity and strength-to-weight ratio. The fuzzy cell edge characteristics assure an excellent bond to face laminates [11]. Globally there has been much concern over climatic changes which have accelerated over the past decade. This has resulted in perceptible global warming, precipitation, flash floods, etc. The root cause of these changes can be attributed to the indiscriminate reduction of green cover in the world, excessive exploitation of non-renewable natural resources, high usage of fossil fuel, etc [11].

1.9.2 Structural Composite

A structural composite is usually made of both homogeneous & composite materials, the properties of which depend not only on the constituent materials properties but also on the geometrical design of the different structural elements. Sandwich panels & laminar composites are two of the most common and important structural composites [19].

1.9.3 Laminar Composites

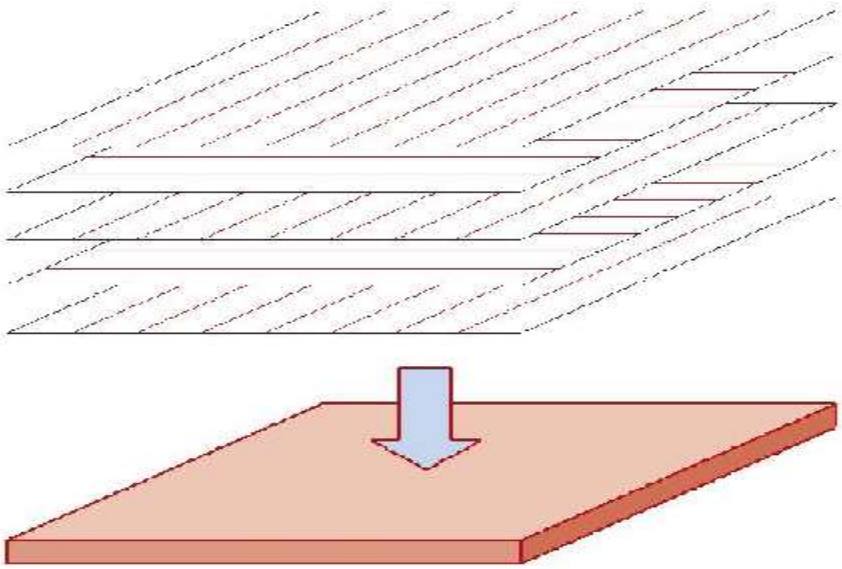

Figure 1.8: The stacking of fiber-reinforced layers for a laminar composite [19]

A laminar composite is made of two-dimensional sheets that have a high-strength direction such as is found in wood and continuous and aligned fiber-reinforced plastics. The layers are stacked and subsequently cemented together such that the orientation of the high-strength direction varies with each successive layer [19]. For example, adjacent wood sheets in plywood are aligned with the grain direction at right angles to each other. Laminations (Figure 1.8) can also be constructed using the material of fabric such as cotton, paper, or woven glass fibers embedded in a plastic matrix. Thus a laminar composite has comparatively high strength in a number of directions in the two-dimensional plane; however, the strength in any given direction is, of course, lower than it would be if all the fibers were oriented in that direction [19].

1.9.4 Dual Laminate

Due to the corrosion resistant nature of FRP, the tank can be made completely from the composite, or a second liner can be used. In either case, the inner liner is made using different material properties than the structural portion (Hence the name dual (meaning two) and laminate (a word commonly used for a layer of a composite material)) [10]. The liner, if made of FRP is usually resin rich and utilizes a different type of glass, called "C-Glass", while the structural portion uses "E-Glass". The thermoplastic liner is usually 2.3 mm thick (100 mils). This thermoplastic liner is not considered to contribute mechanical strength [10].

The FRP liner is usually cured before winding or lay-up continues, by using either a BPO/DMA system, or using an MEKP catalyst with cobalt in the resin [10]. If the liner is not made of FRP, there are multiple choices for a thermoplastic liner [10].

The needs of engineer is to design the tank based on the chemical corrosion requirement of the equipment. PP, PVC, PTFE, ECTFE, ETFE, FEP, CPVC, PVDF are used as common thermoplastic liners [10]. Due to FRP's weakness to buckling, but immense strength against tensile forces and its resistance to corrosion, a hydrostatic tank is a logical application for the composite. The tank is designed to withstand the hydrostatic forces required by orienting the fibers in the tangential direction. This increases the hoop strength, making the tanks anisotropically stronger than steel (pound per pound) [10].

1.10 Sandwich Panels

Sandwich panels, considered to be a class of structural composites, are designed to be light-weight beams or panels having relatively high stiffness's and strengths. A sandwich panel (Figure 1.9) consists of two outer sheets, or faces, that are separated by and adhesively bonded to a thicker core [19]. The outer sheets are made of a relatively stiff and strong material, typically aluminum alloys, fiber-reinforced plastics, titanium, steel, or plywood; they impart high stiffness and strength to the structure, and must be thick enough to withstand tensile and compressive stresses that result from loading [19]. The core material is lightweight, and normally has a low modulus of elasticity. Core materials typically fall within three categories: rigid polymeric foams (i.e., epoxy, polyurethanes), wood (i.e., balsa wood), and paper honeycombs [19].

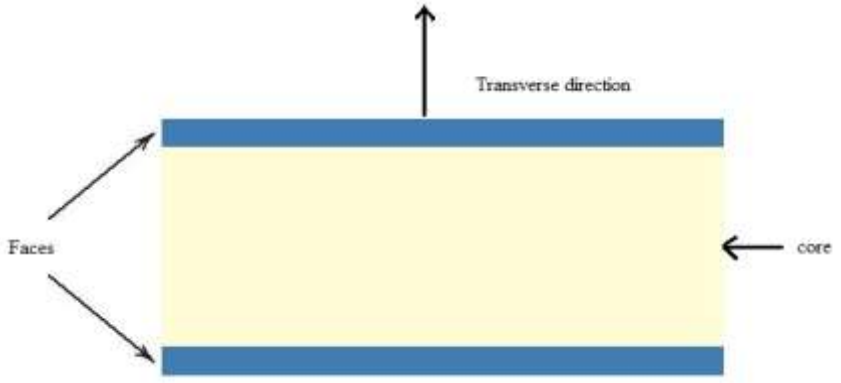

Figure 1.9: Diagram showing the cross section of a sandwich panel [19]

Structurally, the core serves several functions. First of all, it provides continuous support for the faces. In addition, it must have sufficient shear strength to withstand transverse shear stresses, and also be thick enough to provide high shear stiffness (to resist buckling of the panel). (It should be noted that tensile and compressive stresses on the core are much lower than on the faces) [19]. Another popular core consists of a "honeycomb" structure—thin foils that have been formed into interlocking hexagonal cells, with axes oriented perpendicular to the face planes; (Figure 1.10) shows a cutaway view of a honeycomb core sandwich panel [19]. The honeycomb material is normally either an aluminum alloy or aramid polymer. Strength and stiffness of honeycomb structures depend on cell size, cell wall thickness, and the material from which the honeycomb is made. Sandwich panels are used in a wide variety of applications including roofs, floors, and walls of buildings; and, in aerospace and aircraft (i.e., for wings, fuselage, and tailplane skins) [19].

1.11 FRP Vessels and Tanks

FRP Vessels and Tanks are used in multiple applications, requiring a strong, corrosion resistant environment [5].

1.11.1 Scrubbers

FRP Scrubbers are used for scrubbing fluids. In air pollution control technology, scrubbers approach in three varieties they are [5]

- Dry Media [5]
- Wet Media [5]
- Biological [5]

FRP Scrubbers are used for scrubbing fluids. In air pollution control technology, scrubbers come in three varieties, Dry Media, Wet Media, and Biological [5].

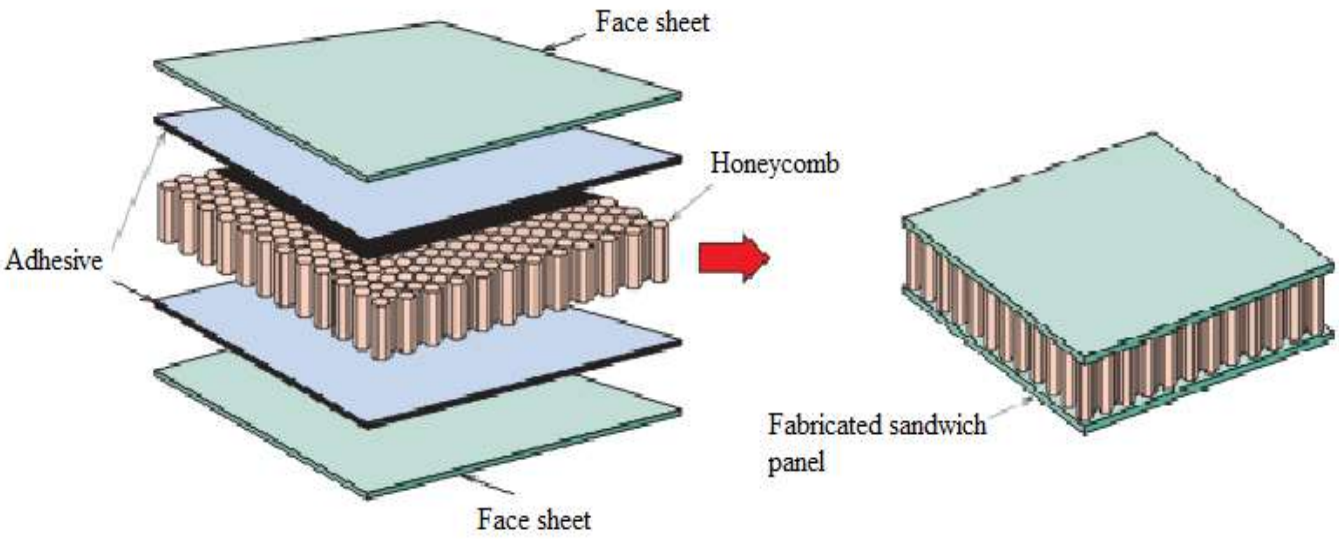

Figure 1.10: Diagram showing the construction of a honeycomb core sandwich panel [19]

1.11.2 Dry Media

Dry media typically involved a dry, solid media (such as activated carbon) suspended in the middle of the vessel on a system of beam supports and grating. The media controls the concentration of a pollutant in the incoming gas via adsorption and absorption [5].

These vessels have several design constraints. They must be designed for [5]

- Unloading and Reloading the media [5]
- Corrosive effects of the fluid to be treated [5]
- Internal and External Pressure [5]
- Environmental Loads [5]
- Support Loads for the grating and support system [5]
- Lifting and Installing the Vessel [5]
- Regenerating the media inside the vessel [5]
- Internal Stack supports for a dual bed construction [5]
- Redundancy for preventative maintenance [5]
- Demisting to remove liquids that degrade the dry media [5]
- Condensate removal, to remove any liquid that condenses inside the vessel [5]

1.11.3 Wet Media

Wet media scrubbers typically douse the polluted fluid in a scrubbing solution. These vessels must be designed to more stringent criteria. The design constraints for wet media scrubbers typically include [5]:

- The corrosive effects of the polluted fluid and the scrubbing solution [5]
- The high pressures and loading of a spray system [5]
- Aerodynamics of the internal media to ensure that there is no bypass [5]
- Internal Support systems [5]
- Reservoir of scrubbing fluid for recirculation [5]
- Internal and External Pressure [5]
- Environmental Loads [5]

In the case of a decarbonator, used in reverse osmosis systems to limit the concentration of gases in the water, the air is the scrubbing fluid and the sprayed liquid is the polluted stream. As the water is sprayed out of the scrubber, the air strips the aqueous gasses out of the water, to be treated in another vessel [5].

1.11.4 Biological

Biological scrubbers are structurally identical to the wet media scrubbers, but vary in their design. The vessel is designed to be larger, so the air moves slower through the vessel. The media is designed to encourage biological growth, and the water that sprays through the vessel is filled with nutrients to encourage bacteria to grow. In such scrubbers, the bacteria scrub the pollutant. Also, instead of a single, large support system (typically 10 feet depth of media for chemical scrubbers), there are multiple stages of media support, that can change the design requirements of the vessel [5].

1.11.5 Tanks

A typical storage tank made of FRP has an inlet, an outlet, a vent, an access port, a drain, and an overflow nozzle. However, there are other features that can be included in the tank. Ladders on the outside allow for easy access to the roof for loading [5]. The vessel must be designed to withstand the load of someone standing on these ladders, and even withstand a person standing on the roof. Sloped bottoms allow for easier draining. Level gauges allow someone to accurately read the liquid level in the tanks [5].

1.12 Semiconductor Strain Gauges

Semiconductor strain gages are not widely used in experimental stress analysis and there are a number of reasons for this [19]:

- The non-linear characteristics of the semiconductor strain gage call for measurement correction demanding high accuracy [19]
- Semiconductor strain gages are substantially more expensive than metal types [19]
- Even when the greater sensitivity is taken into account, the adverse temperature dependent effects are more severe with semiconductor strain gages than with metal ones and these effects are more difficult to compensate [19]
- Handling is more difficult due to the semiconductor's brittle nature [19]

On the other hand the high sensitivity is a reason for using semiconductor strain gages for the measurement of very small strains. The large signal given by this type of strain gage is of particular advantage in the presence of strong interference fields [19].

1.13 Displacement Transducer

A measuring transducer that converts a linear or angular displacement into an electric, mechanical, pneumatic, or other signal suitable for recording long distance transmission. Some transducers which has been used for displacement transducers Capacitance sensors, inductance sensors, transformers, resistive, stringed photoelectric jet, induction and electrodynamic transducers as well as coding disks [19].

A distinction is made between displacement transducers for small displacements (from several microns to several centimeters) and for large displacements (from tens of centimeters to several meters). Greater displacements are measured by means of travelling transducers. The greatest sensitivity for the measurement of small displacements is provided by photoelectric sensors, capacitance sensors and some types of inductance sensors [19].

1.14 Advantage of Composites

The greatest advantage of composite materials is strength and stiffness combined with lightness. By choosing an appropriate combination of reinforcement and matrix material, manufacturers can produce properties that exactly fit the requirements for a particular structure for a particular purpose [13].

Modern aviation, both military and civil, is a prime example. It would be much less efficient without composites. In fact, the demands made by that industry for materials that are both light and strong has been the main force driving the development of composites [13].

It is common now to find wing and tail sections, propellers and rotor blades made from advanced composites, along with much of the internal structure and fittings. The airframes of some smaller aircraft are made entirely from composites, as are the wing, tail and body panels of large commercial aircraft [13].

In thinking about planes, it is worth remembering that composites are less likely than metals (such as aluminum) to break up completely under stress. A small crack in a piece of metal can spread very rapidly with very serious consequences (especially in the case of aircraft). The fibers in a composite act to block the widening of any small crack and to share the stress around [13].

The right composites also stand up well to heat and corrosion. This makes them ideal for use in products that are exposed to extreme environments such as boats, chemical-handling equipment and spacecraft. In general, composite materials are very durable [13].

Another advantage of composite materials is that they provide design flexibility. Composites can be moulded into complex shapes – a great asset when producing something like a surfboard or a boat hull [13].

1.15 Limitations

Weak spots of perpendicular fibers can be used for natural hinges and connections, but can also lead to material failure when production processes fail to properly orient the fibers parallel to expected forces. When forces are exerted perpendicular to the orientation of fibers the strength and elasticity of the polymer is less than the matrix alone [12].

In cast resin components made of glass reinforced polymers such as UP and EP, the orientation of fibers can be oriented in two-dimensional and three-dimensional weaves. This means that when forces are possibly perpendicular to one orientation, they are parallel to another orientation; this eliminates the potential for weak spots in the polymer. The downside of composites is usually the cost. Although manufacturing processes are often more efficient when composites are used, the raw materials are expensive [12].

2. PROJECT DESCRIPTION

2.1 Materials

The face sheets were made-up from glass fiber R25H which is usually made of Advantex glass and polyvinylester resin Synolite 8388-P-1 and usually designed for filament winding processes. Different standard tests were performed at room temperature in order to determine the mechanical properties of separate sandwich components and 2 mm/min rate of loading using the universal testing machines and the measuring system HBM (Hottinger Baldwin Messtechnik GmbH) [37], HBM measuring system involved with displacement and force transducers, SPIDER-8 which is a four-channel measuring amplifier and a computer with Catman Express software [37]. Tension test is carried out on a sheet of GFRP comprising one-ply glass filament and polyvinylester resin which was cured having an average thickness of was 0.9 mm. The specimens were prepared in the longitudinal and in transverse directions. The sheet of GFRP undergoes compression test too [37]. A sheet of thickness of 10 mm comprising 11 plies of glass filament was made. Sandwich structure in (Figure 2.1): glass fiber with polyvinylester resin composite face sheets; polyvinylester resin impregnated with recycled paper hexagonal honeycomb core [37].

Figure 2.1: Composite sandwich structure specimens

2.2 Experimental Testing Conditions

The strength analysis consists of performing the experimental method, finite element method (Ls Dyna) and analytical results. From the results of the methods making a conclusion about the stress and behavior of the composite sandwich structures.

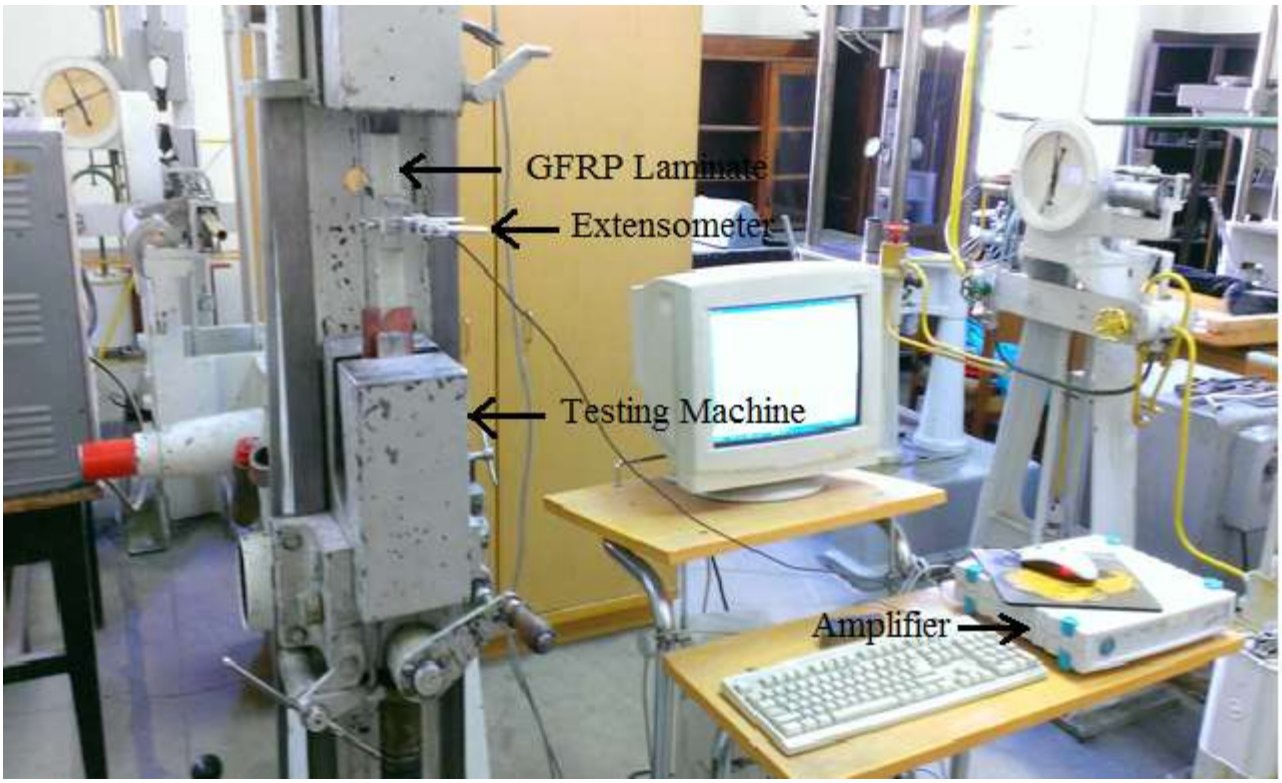

Figure 2.2: Experimental setup of testing specimens

Test performed According: EN ISO 527-4 Plastics. Determination of tensile properties. Part 4: Test conditions for isotropic and orthotropic fiber-reinforced plastic composites.

Test conditions: Temperature: 20°C.

Specimens: Specimens cutted from the tank diameter of 1.8 m

Measuring Devices: Force transducers 100 kN±200 N, 10kN ±10N, displacement transducer 20±0,04 mm, extensometer base 50, range ±2,5 mm.

2.3 Measurement of Fiber Volume Fraction

The fiber volume fraction of the E glass fiber facesheets was determined by using burn-out test method, samples of about 0.1-0.10 g. of facesheet was burned off in a high temperature oven at about 750°C for about an hour. The burn-out test method is also used to determine the number of layers in the laminate. The remaining fiber mass was weighed and the volume of the fiber was calculated by dividing the mass of the fiber by the density of the fiber material. The fiber volume fraction (V_f) has been calculated as below;

$$V_f = \frac{v_f}{v_f + v_m} \times 100 = \frac{\frac{m_f}{\rho_f}}{\left(\frac{m_f}{\rho_f} + \frac{m_m}{\rho_m}\right)} \times 100 \tag{2.1}$$

where v_f and v_m are the volume of fiber and matrix, m_f and m_m are the mass of fiber and matrix and ρ_f and ρ_m are the density of fiber and matrix, respectively.

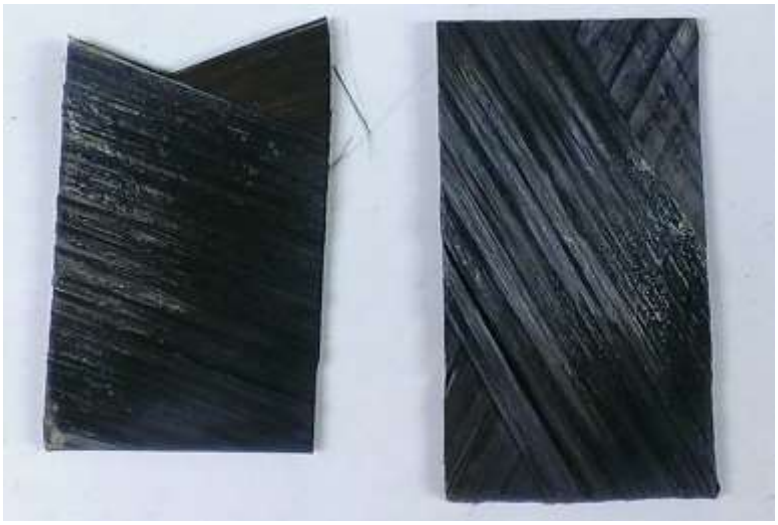

Figure 2.3: Facesheet of composite sandwich structure after burn out test

2.4 Tension Test on GFRP Laminate

2.4.1 Specimen Preparation and Experimental Setup

Figure 2.4: Tensile test specimen before the test

The tensile strength and elastic modulus of the composite facesheets were obtained by using tensile test technique, EN ISO 527-4, using a diamond saw at least five specimens were prepared. The first step, verification of the numerical composite model by simulating the uniaxial tensile test of facesheets was performed. Test specimens were sectioned from the composite panels. The laminate code was [±65^o /90^o], the layers of angle of ply equal to 90^o and ±65^o had thicknesses of 0.9 mm and 0.8 mm. The total thickness of the facesheet was equal to 3.5 mm [37].

In the tension test, the facesheet of the GFRP specimen is prepared and the specimens having four different angles 0^o, 30^o, 60^o, 90^o. The specimen is placed in the testing machine. An extensometer is fixed in the facesheet to find out the elastic behavior, plastic behavior and breaking point of the specimen. The displacement transducer is used to measure the displacement in the facesheet. The force transducer measures the load applied in the material. The testing is done for at least five different specimens in each angles to find out the accurate properties of the facesheets. The results from the tensile test is plotted against force versus displacement (Figure 4.10).

Figure 2.5: Tensile test specimen during the test

The tensile strength (σ) values were calculated by the following equation;

$$\sigma = \frac{F}{A} \tag{2.2}$$

where F is the ultimate load, and A is the cross sectional area of the specimen. Elastic modulus was obtained from the initial slope of stress (σ) - strain (ε) curves based on the equation below;

$$E = \frac{\sigma}{\varepsilon} \tag{2.3}$$

Figure 2.6: Tensile test specimen after the test (30^{o})

2.5 Bending Test on GFRP Sandwich Structure

2.5.1 Specimen Preparation and Experimental Setup

Figure 2.7: GFRP Specimen for bending test

By simulating three-point bending test the verification of the sandwich structure model was performed. The process includes various effective steps. The first step is an experimental test which was carried out very efficiently. The specimens is placed in the mechanical testing machine and these specimens were cutout from the large sections of the cylinder. The load applied on the specimen is at the rate of 2 mm/min. The load is applied in the center of the specimen at that time the two ends of the specimen is fixed [37]. The force versus deflection is also measured. The dimensions of the bending test specimens are: width 60 mm, the thickness of top facesheet 3.0 mm, the thickness of bottom facesheet 2.4 mm, the core thickness 10 mm, the sandwich thickness 15.4 mm and the distance between supports is 200 mm [37].

The windings are normally done in longitudinal and circumferential direction. In each direction five different specimens are prepared. The load is applied on specimen until the bonding between the core and facesheet breaks due to the force applied. The point to which the load withstands defined as the maximum load withstanding capacity of the GFRP specimen. At this peak point the core material fails due to the load applied. Depending upon the results obtained the specimens are compared with each other and a suitable force versus deflection curve is suited for the calculations (Figure 4.18).

2.6 Compression Test on GFRP Cylinder Ring

2.6.1 Specimen Preparation and Experimental Setup

The verification of the model has been performed by experimental test of ring compression. Six rings of the same dimensions and structure were made and tested.

Figure 2.8: Experimental testing on GFRP Cylinder Ring

On the hollow cylinder ring has to be tested by the compression test. A hollow cylinder of internal diameter D_c = 600mm and width b_c = 196 mm FE model was designed. A sandwich GFRP composite was defined as a honeycomb core the wall of the cylinder [37]. The laminate code of internal facesheet had three layers which was [±65º/90º]. There was four layers on the external facesheet and the laminate code was $[\pm 65^{o}]_2$ [37]. The thickness of the facesheet was 0.9 mm and 0.75 mm and the layers of angle of ply equal to 90º and ±65º. The external facesheet thickness was of 3.0 mm. The thickness of the core was equal to 10 mm and the total thickness of internal facesheet was equal to 2.4 mm. The FE modelling results were measured for force and deflection (Figure 4.20).

3. MODELING COMPOSITE SANDWICH STRUCTURES

3.1 Modeling Sandwich Structures

Mechanics can be divided into three major areas [30]:

a) Theoretical

b) Applied

c) Computational

The fundamental laws and principles of mechanics is regarding with the Theoretical mechanics. The mathematical models of physical phenomena and to establish scientific and engineering applications uses the theoretical knowledge of applied mechanics. The simulation through numerical methods on computers solves problems for computational mechanics [30].

The computational mechanics can be distributed into numerous branches according to the physical scale of the problem [30]:

a) Nanomechanics and micromechanics

b) Continuum mechanics

c) Systems

The design and production of materials and micro devices were widely used for technological applications and concerns about the crystallographic and granular levels of matter by micromechanics and the molecular and atomic levels were dealt with the nanomechanics. In order to analyze and design structures the main parameters used is the microstructure in solid and fluid mechanics by using the continuum mechanics. The structures are the most general ideas and with mechanical objects that perform a noticeable function [30].

Continuum mechanics problems can be divided into two other categories [30]:

a) Statics

    i. Linear

    ii. Nonlinear

b) Dynamics

    i. Linear

    ii. Nonlinear

The dependency for calculations of inertial forces and derivatives with respect to time in dynamic cases in dynamic cases. According to the case of interest there is no time dependence for statics. The static problems were dealt with linear static analysis with which the response is linear in the cause and effect sense. Problems outside this area are classified as nonlinear [30].

Another classification of the static analysis of continuum mechanics is based on the spatial discretization method by which a problem can be converted to a discrete model of finite number of degrees of freedom [30].

Finite Element Method (FEM)

The finite element method is generally used for linear problems. The finite element methods is undisputable for nonlinear problems. In (Figure 3.1) the steps in the finite element modeling can be seen [30].

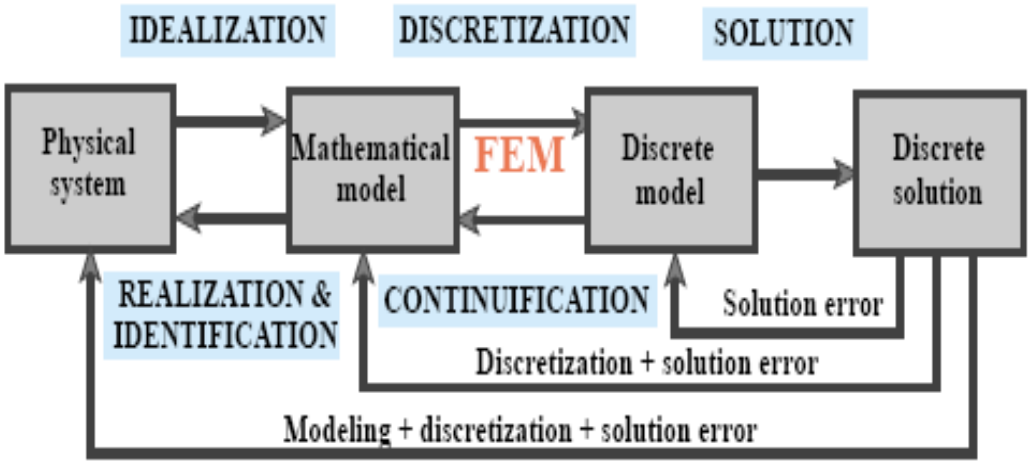

Figure 3.1: A diagram of the physical simulation process [30]

The complexity in analysis of composite structures allows the designer to vary up the layup configuration has a greater flexibility. Compared with the traditional engineering materials the modeling of composite materials is more difficult [30]. In the conventional materials the damage and failure in laminated composites are very complex. In the case of finite element modeling of composite laminates is done by rnacromechanical and micromechanical modeling in terms. The volume fraction of the fibers and the individual properties of the constituent materials were the properties of composites as strength and stiffness [30].

3.1.1 Micromodelling

The same matrix material so that it can be isolated from the whole composite by a arrays of parallel fibers by the volume. The individual properties of the fiber and matrix symbolic volume element has the same fiber volume fraction as the composite laminate. The volume element can also used as a demonstrative approach can be used as a replacement for the difficult microstructure of the composite [31].

The separate elements effective properties can be obtained with this micromechanical approach. The overall response of the composite used in the symbolic volume element model has separate elements. The fiber and matrix level provides more physical information by this method [31]. The damage mechanisms and predicting damage progression inside the composite laminates is important for composites. The combination to select the best methods and the material properties allows the designers to combine different material properties [30].

3.1.2 Macromodelling

The macromechanical approach is concerns with the influences of each ply to the overall properties and the properties of the fiber and matrix are averaged to produce a set of homogenous, orthotropic properties [31]. The macromechanical approach has the advantage of simplicity, it is not possible to identify the stress-strain states in the fiber, matrix and their interface. In other turn the micromechanical approach, the elements and their interface can be definitely considered to forecast the overall response of the composite as well as the damage beginning and spread in the composite [31].

Due to the several layers of composites with different orientation and properties the level of difficulty increases for composite laminate because of the stacking. The stress-strain relations of a composite laminate can be obtained and coupling mechanisms between in-plane and out of plane deformation modes can be discovered [31]. The stress and material strength can be predicted for unidirectional fiber reinforced composite by the macromechanical approach. The criteria are based on the average composite stress strain states used to detect failure are maximum stress, maximum strain, Tsai-Hill, Tsai-Wu. The fiber and matrix materials behavior will not be considered in the macromechanical approach [31].

3.1.3 Classical Lamination Theory

A laminate is shown in (Figure 3.2). The mechanical behavior of composite laminates can be obtained by the macromechanical approach of the classical laminate theory. A structural element contains two or more laminae that is bonded together is called a laminate [33]. The effects has to be minimized with the low transverse properties and with this the maximum advantage has to be obtained. The orthotropic laminated composite materials have good properties in the direction of the reinforcing fibers, but poor properties perpendicular to the fibers. To match the design needs the plies or lamina directions are oriented in several ways with the effective properties of the laminate (Figure 3.3) [33].

The arbitrary angles of the laminate serves as a procedures enable the analysis of laminates that have individual laminae orientations. The stiffness of a composite material obtained from the properties of the fundamental laminae for the structural analysis [33]. As a result the overall behavior of multidirectional laminate is a role of the properties and stacking order of the individual layers. This behavior of the laminate is called as the classical lamination theory. The laminates where separate plies display inelastic reply, additional inelastic strains terms are essential [33].

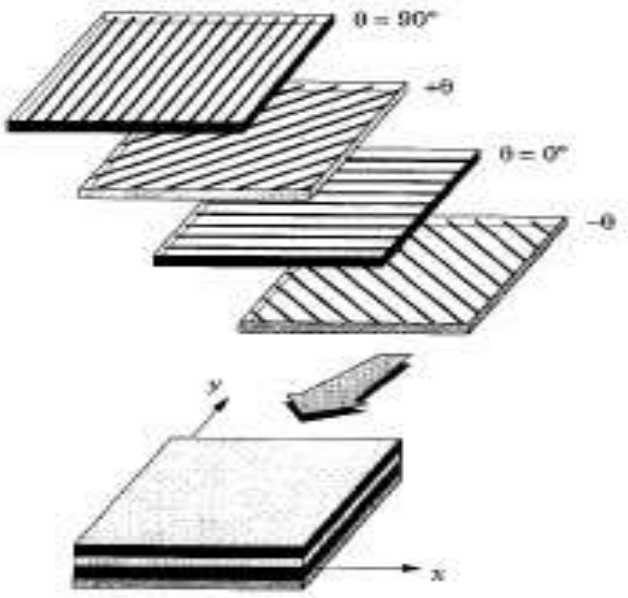

Figure 3.2: A laminate with different fiber orientations [33]

Figure 3.3: The angle of ply in GFRP laminate

To explain bending stiffness of a laminate in the laminate thickness it is essential to have ideas about the variation of stress and strain. In this theory the laminate is expected as perfectly attached lamina in load applications [34]. The bonds are expected to be infinitesimally thin as well as non-shear deformable. The displacements are continuous through the lamina boundaries that no lamina can slip. The resultant forces and moments acting on a laminate are got by the integration of the stresses in each layer or lamina through the laminate thickness [34].

3.2 Numerical Modeling of Composite Sandwich Structures

The LS - DYNA was used for the finite element analysis of the composite sandwich structure. The finite element analysis technique was used to model the composite sandwich structures and its elements by the mechanical behaviors [34]. Composite materials are difficult to model because of their different orthotropic properties, so proper element types must be selected, layer configuration must be given, failure criteria must be defined and lastly modeling and post-processing tasks has to be done [34]. The most important characteristic of the composite materials is its layered configuration. The properties of the layers have to be specified individually or defined constitutive matrices that are related with the generalized forces, moments and strains by using proper element types [34].

The element is defined by layer thicknesses, layer material direction angles, orthotropic material properties and allows up to 100 layers. The layer configuration is defined from bottom to top in the positive z direction of the element coordinate system [34].

Failure criteria are also defined for the structures in order to find out whether a layer is failed due to the applied loads. There are four widely known failure criterias, they are [34]:

- Chang and Chang Failure Criterion
- Hashin's Failure Criterion
- Tsai-Hill Failure Criterion
- Tsai-Wu Failure Criterion

Failure criteria are orthotropic, therefore it must be taken into account that failure stress and strain values must be given as an input for the program. In this study Chang and Chang, Hashin's failure criterion is being applied to the structures [34].

3.2.1 Modeling of Facesheets

The MAT 54 (*MAT_ENHANCED_COMPOSITE_ DAMAGE) was used to design the GFRP facesheets based on four failure criteria by Chang and Chang was selected [35]. The Nonlinear shear stress parameter (ALPH = 0) and factor for shears term in tensile fiber mode (BETA=1) was not used thus the original criterion of Hashin [36] was selected. The elastic and failure performance by using a ply discount process to reduce the elastic properties of composites can be defined by using the material model MAT54 [37]. The other material models does not achieve the experimental performance by using material models like MAT 22 (*MAT_COMPOSITE_DAMAGE resulting in an agreement between experiment and simulation [37].

The first step is the confirmation of the numerical composite model by performing the uniaxial tensile test of facesheets [37]. The facesheet angle was [$\pm 65^o$ /90^o], the angle of the layers of was equal to 90^o and $\pm 65^o$ have thickness of 0.9 mm and 0.8 mm. The total thickness of laminate was equal to 3.5 mm [37]. The mechanical properties of GFRP laminate used are presented in (Table 4.1). The numerical results of elastic behavior showed good coincidence with experimental stress–strain curve (Figure 4.3a and 4.3b) [37].

Table 3.1: Failure properties of composite element for LS-Dyna material model MAT54 [37]

Component	DFAILM	DFAILS	DFAILT	DFAILC	EFS	FBRT	TSMD
GFRP	0.028	0.03	0.0172	- 0.028	_	0.5	_
Glue	_	_	_	_	4.5 e–4	_	0.2
Core	_	_	_	_	4.5 e–4	_	0.2

3.2.2 Modeling of Sandwich Structure

The FE code LS-DYNA v.971 R7.0.0 was used to model composite sandwich structures. The GFRP honeycomb core the material model MAT 54 (*MAT_ENHANCED_COMPOSITE_DAMAGE) based on four failure criteria by Chang and Chang was selected [35]. Honeycomb sandwich structures GFRP can be modelled in several ways using shell elements for both the facesheets and the hexagonal cells, using shell elements for the facesheets and solid elements for the core, using layered thick shell elements or using layered thin shell composite elements [37]. The shell is expected to be made of a corresponding single similar layer. As the debonding failure mode between the core and facesheet has occurred in the experiment testing the simulation of the core debonding phenomena should be done using 3D solids elements and Tiebreak contact pair for the connection with the shell elements of the facesheet [37]. In order to save computational time for large-scale models, thin shell composite elements with single layer assumption were chosen to model the honeycomb sandwich structure [37].

The quasi-static tests were performed by an explicit analysis because in an implicit analysis the progressive failure mode gives inappropriate results [37]. FE model of composite shell elements do not allow simulation of debonding failure mode but the failure criteria allows a decrease of the stiffness of the glue and core layers which shows behavior of cylinder similar to the debonded structure [37]. A constant loading rate of 100 mm/s was applied for all simulation cases [37].

FE mesh size does not considerably impact the results and for the calibration tests a 2mm size of FE mesh was used [37]. A sandwich structure with facesheets of glass fiber composite and a honeycomb core had been modelled with one Part (*Part_Composite) [37]. The attachment among the honeycomb core and facesheets has been modelled by inserting glue layers. In the real sandwich structure, the glue or adhesive as separate material is not used but adhesion is achieved due to the facesheet resin adhesion

properties [37]. The glue properties for the numerical model were defined as the mechanical properties of Synolite 8388-P-1 resin (Young's modulus and tensile strength were 3.7 GPa and 14 MPa, respectively) [37].

A sandwich structure showing the angle of fibers orientation is presented in (Figure 3.2). The continuous failure abilities of the mdoel was used to select the material model MAT 54 in LS-Dyna. The tension test results has been used as material properties for the GFRP plies [37]. The honeycomb core and glue layer was modelled with the MAT 54 model, but the main criterion has been chosen as effective failure strain (EFS) (Table 3.1), which immediately reduces the ply stresses to zero. For glue and core layers, the transverse shear maximum damage (TSMD = 0.2, see Table 3.1) coefficient was used to decrease the transverse stiffness [37].

3.2.3 Modeling of GFRP Cylinder Ring

Using the obtained data for materials properties, a numerical FE model of an annular section of the cylinder (ring) was designed. With the aim of obtaining the stress, the simplest approach has been chosen to simulate the behavior of radially compressed annular cylinders [37]. The FE model which defined a hollow cylinder of internal diameter D_c = 600 mm and width b_c = 196 mm, was designed. The wall of the cylinder was defined as sandwich GFRP composite with a honeycomb core [37]. The internal facesheet had three layers; the laminate code was [±65°/90°]. The external facesheet had four layers; the laminate code was $[\pm 65^{o}]_2$ [37]. The layers of angle of ply equal to 90° and ±65° had thicknesses 0.9 mm and 0.75 mm, respectively [37]. The total thickness of the internal facesheet was equal to 2.4 mm; the external facesheet thickness was of 3.0 mm. The thickness of the core was equal to 10 mm [37].

4. RESULTS AND DISCUSSION

The properties of honeycomb core material, facesheet material and composite sandwich structure are presented in (Table 4.1 and Table 4.2). In addition, comparisons of numerical and experimental results on the mechanical properties are given. The standards for the experimental testing are ISO 527, ISO 604, and ISO 844. The (Table 4.1) shows the mechanical properties that were obtained during the tensile test of the laminate.

Table 4.1: Mechanical properties of the GFRP

Mechanical Properties	Value	Unit
Longitudinal tensile strength, X_T	645	MPa
Transverse tensile strength, Y_T	19.6	MPa
Longitudinal compressive strength, X_c	248	MPa
Transverse compressive strength, Y_c	48.2	MPa
Longitudinal Young's modulus, E_1	37.5	GPa
Transverse Young's modulus, E_2	7.32	GPa
Poisson's ratio, v_{12}	0.28	_
Poisson's ratio, v_{21}	0.05	_
Shear modulus, G_{12}	3.79	Gpa
In-plane shear strength, S_{12}	23.0	Mpa

Table 4.2: Mechanical properties of the paper honeycomb

Mechanical Properties	Value	Unit
Young's modulus, E_{h1}	10	MPa
Young's modulus, E_{h2}	2.9	MPa
Young's modulus, E_{h3}	25	MPa
Shear modulus, G_{h13}	235	MPa
Compression strength,σ_{hU}	0.48	MPa
Shear strength, τ_{hU}	0.64	MPa

4.1 Fiber Volume Fraction

Fiber volume fraction of the produced E-glass fiber composite facesheets was measured by matrix burn-out test. The average fiber volume fraction was measured as 43% for the composite facesheets. There was four layers of glass fibers with different angles of orientation in the laminate. The elastic modulus for various fiber volumes is given in the (Figure 4.1).

Table 4.3: Recommended use of fiber volume fraction [41]

Type of Reinforcement	Range of Fibre Volume Fraction	Common Value of Fibre Volume Fraction (%)
Unidirectional	40-70	65
Woven	35-55	45
Random	10-30	20

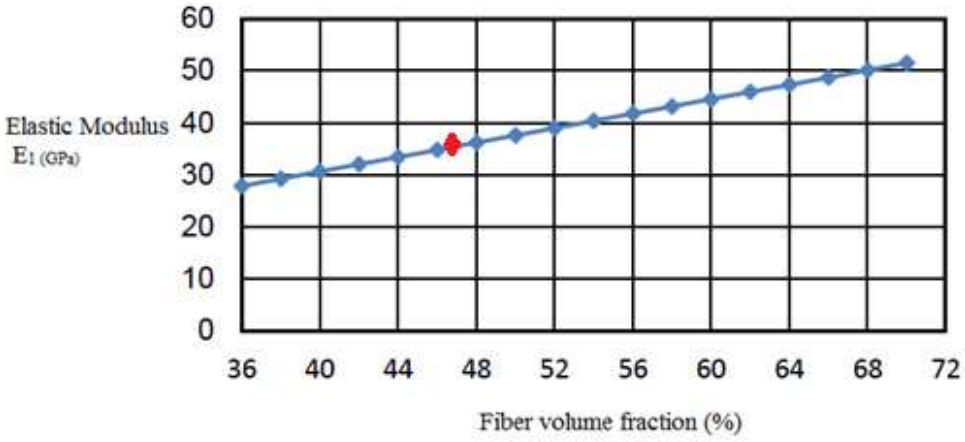

Figure 4.1: Elastic modulus E_1 at various fiber volume fractions [41]

The fiber volume fraction for the unidirectional GFRP specimens can be obtained from the (Table 4.3). The red marking on the graph shows the average value of fiber for the obtained Young's modulus. The common use of fiber volume fraction for unidirectional lamina ranges from 40% to 70%. The recommends a range of possible fiber volume fractions for different reinforcement forms as shown in (Table 4.3).

4.2 Tension Test on GFRP Laminate

4.2.1 Experimental Results of Tension Test of GFRP with Differently Oriented Layers

The tension test is done on the laminates that were cutted from the composite sandwich structure using a diamond saw. For each angles five different specimens were prepared from the composite structure. The total thickness of the facesheet was equal to 3.5 mm. The laminate has four different types of angles they are shown in (Figure 4.2). The facesheet is fixed at both the ends and the load is applied in the middle of the facesheet. The result from the experiment is plotted as force vs displacement.

Table 4.4: Results obtained from experimental calculations of GFRP laminates [±65 / 90]

Specimen No	b mm	t mm	Fmax kN	E GPa	Sm MPa		Specimen No	b mm	t mm	Fmax kN	E GPa	Sm MPa
1-0-T	25.6	3.4	21.3	31.6	245.8		1-60-T	25.5	3.8	1.66	10.2	17.2
2-0-T	25.4	3.5	30.7	22.8	345.6		2-60-T	25.1	4.1	1.72	8.5	16.7
3-0-T	25.8	4.2	58.2	31.2	537.2		3-60-T	25.9	3.8	1.77	7.4	17.8
4-0-T	25.6	3.6	52.8	26.7	573.9		4-60-T	25.7	4.9	1.68	7	13.3
7-0-T	25.2	3.4	24.5	23.1	286.2		5-60-T	25.6	3.7	1.62	12.2	17.1
8-0-T	25.2	3.3	39.4	28.9	474.6		Average				9.06	16.42
9-0-T	25.9	3.6	22.5	30.1	241.6		STVDEV				1.95	1,59
Average				27.8	386.4		CONFIDENCE				1.44	1.18
STVDEV				3.7	140.3							
CONFIDENCE				2.7	103.9							
1-30-T	25.9	3.6	15.5	22	166.7		1-90-T	25.6	3.4	1.34	10.8	15.5
2-30-T	25.9	3.6	15.7	19.4	169		2-90-T	25.7	4.9	1.24	4.9	9.8
3-30-T	25.9	4.1	16.2	22	153.5		3-90-T	25.7	3.3	1.17	9.1	13.8
4-30-T	25.9	4.1	17.3	18.8	163.4		4-90-T	25.7	3.4	0.55	7.5	6.4
5-30-T	25.1	3.6	16.1	21.6	179		5-90-T	25.3	3.4	0.71	8.7	8.2
Average				20.76	166.32		6-90-T	25.7	4.8	1.46	7.1	11.91
STVDEV				1.53	9.23		Average				8.07	10.935
CONFIDENCE				1.13	6.83		STVDEV				1.99	3.44
							CONFIDENCE				1.47	2.55

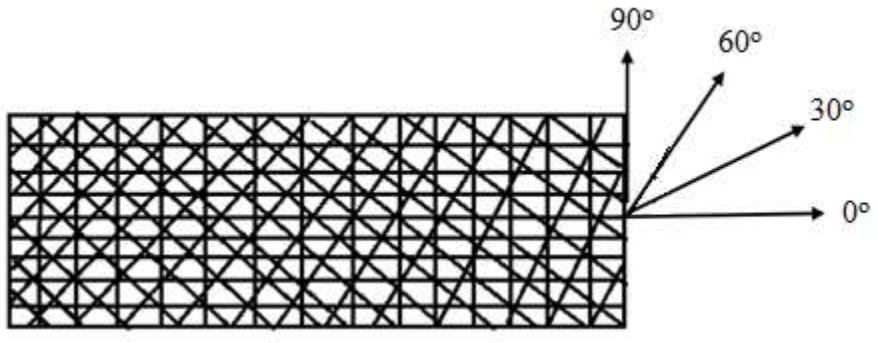

Figure 4.2: Represents the angle of winding of fibers 0°, 30°, 60° and 90°

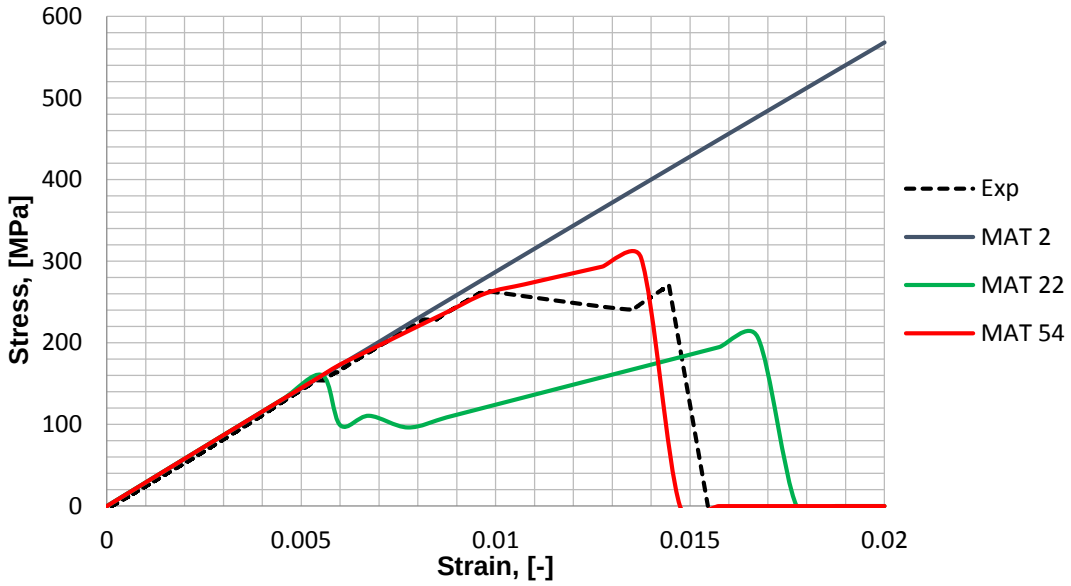

Figure 4.3a: Tensile stress–strain curves of GFRP laminates

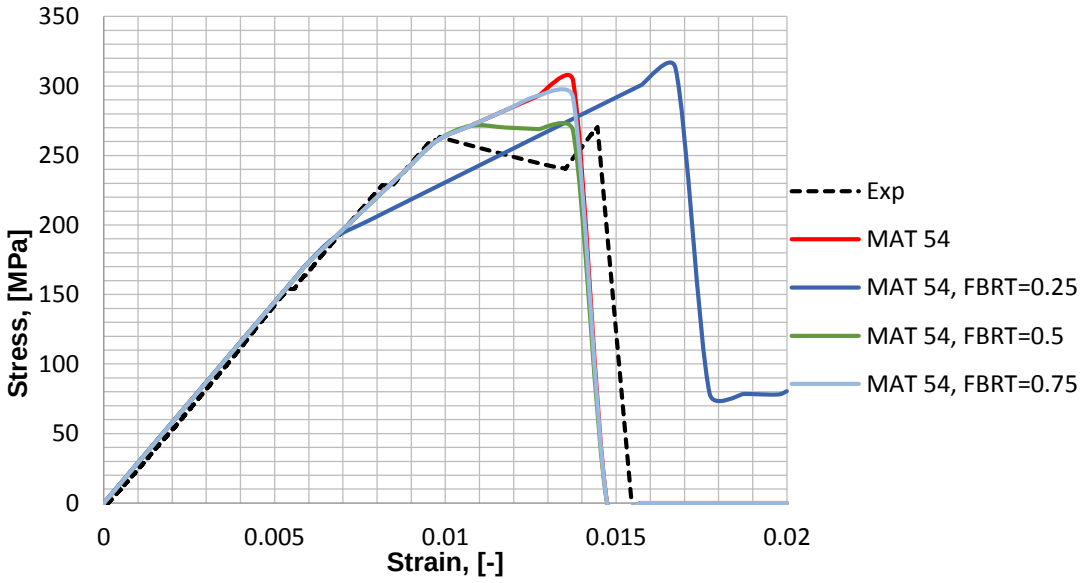

Figure 4.3b: Tensile stress–strain curves of GFRP laminates

The (Figure 4.3a) represents the angles of the laminates that were experimentally tested and the simulation of the different types of materials in the LS-DYNA software. The experimental laminate is verified with different material in simulation such as MAT 2, MAT 22 and MAT54 [37]. When the strength criteria is reached, the 'plastic' behavior starts and continues until failure strain is reached. Tensile (DFAILT) and compressive (DFAILC) failure strain in fiber direction, failure strain in matrix

direction (DFAILM) and shear failure strain (DFAILS) were experimentally determined and used to simulate the progressive failure of the ply [37]. Some parameters like fiber tensile strength softening parameter (FBRT) cannot be obtained experimentally; therefore, it has been determined using virtual testing strategies. The influence of different material models and fiber tensile strength softening parameter can be seen in (Figure 4.3b) [37]. The best coincidence gives curve 6 and in subsequent work the value of FBRT = 0.5 has been used. In (Figure 4.3a), the coincident behavior of curves 4 and 7 represented MAT 54 model with FBRT parameters equaling 1.0 and 0.75 respectively, which means that after reaching the compressive matrix criteria, double decreasing of fiber tensile strength should be initiated [37].

4.2.2 Finite Element Methods for Tension Test of GFRP with Differently Oriented Layers

4.2.2.1 Ls – Dyna

The (Figure 4.4) shows the designed GFRP laminate with fixed nodes and load applied nodes. The angles of the laminate is changed with different angles and different behavior of the laminate is obtained. The laminate code was [± 65^o /90^o], the layers of angle of ply equal to 90^o and ± 65^o had thicknesses of 0.9 mm and 0.8 mm. The total thickness of the facesheet was equal to 3.5 mm.

Figure 4.4: GFRP laminate with fixed nodes and loads applied nodes

The (Figure 4.5, 4.6, 4.7, 4.8) shows the laminate with different angles of fiber direction. Uniaxial tensile test boundary conditions were defined in the code as clamped at one end. On the opposite end the laminate is extended and the deformation was applied in the x direction. The red zone in the figure denotes

the weak zones in the facesheet and the failure of the facesheet starts from this zone. The crack continues to grow and the breakage finally occurs in the GFRP facesheet when the maximum load is applied.

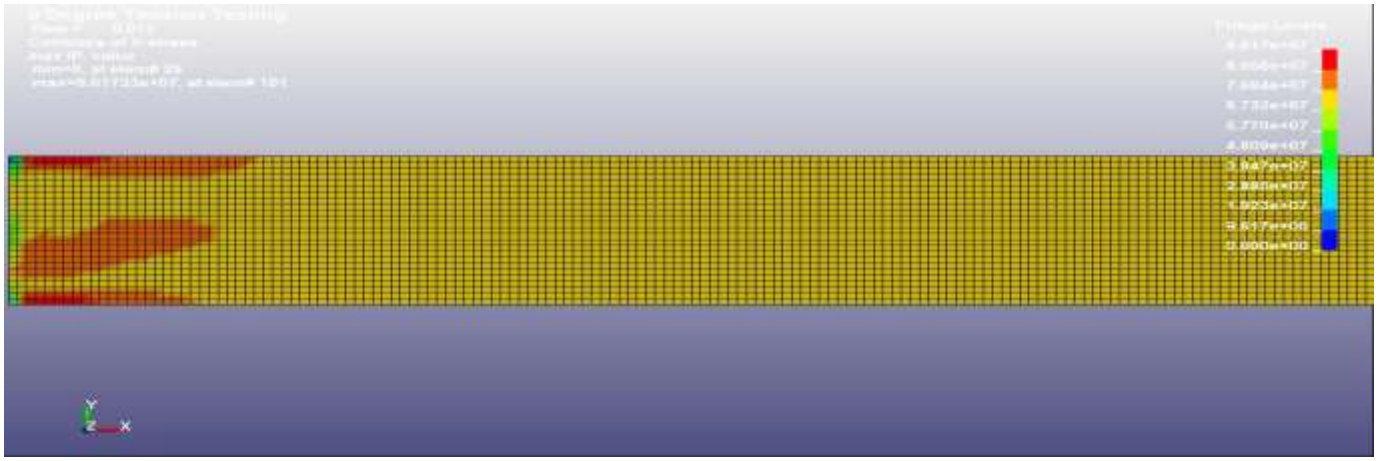

Figure 4.5: Stress on x direction 0^o GFRP laminate

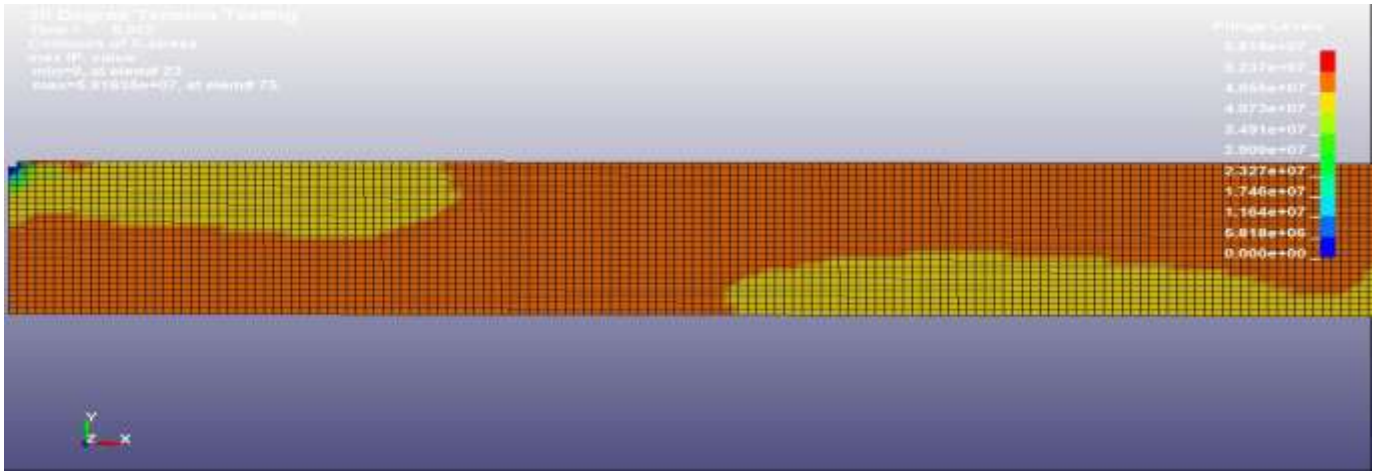

Figure 4.6: Stress on x direction 30^o GFRP laminate

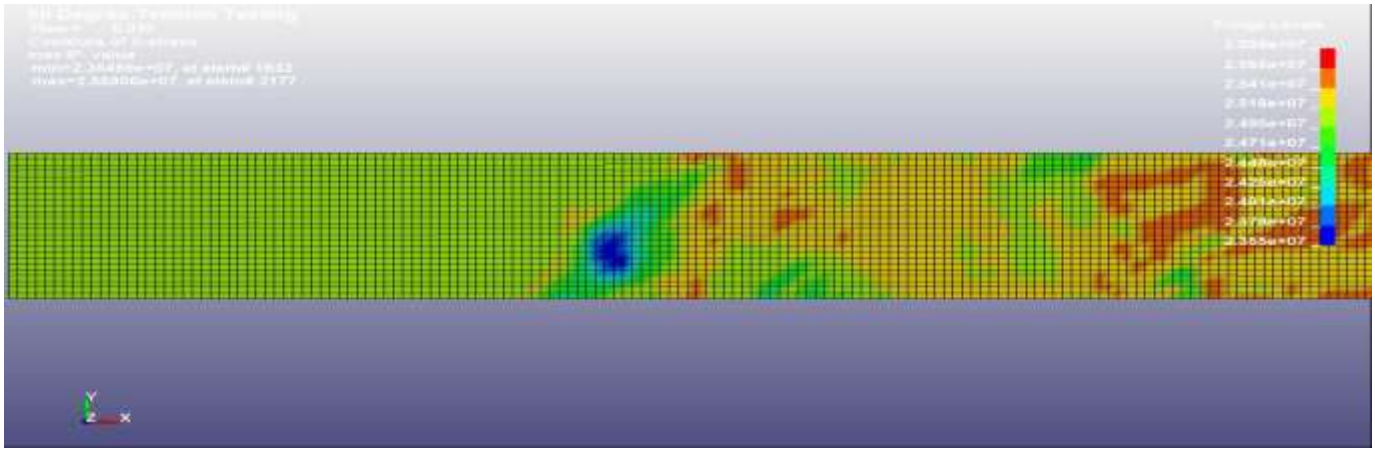

Figure 4.7: Stress on x direction 60^o GFRP laminate

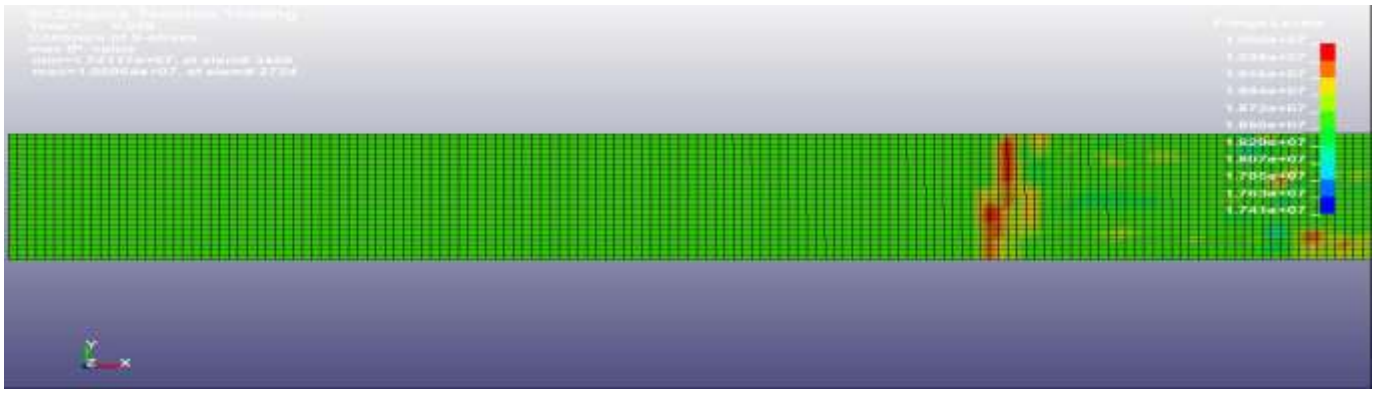

Figure 4.8: Stress on x direction 90^{o} GFRP laminate

4.2.3 Analytical Method for Tension Test of GFRP with Differently Oriented Layers

The analytical method involves the calculation of the shear modulus of the GFRP specimen by using the mat lab software program and comparing the obtained results with the experimental values. The first step is writing of the program with the parameters which are known while designing the model is used. The thickness (t) of the specimen is measured four different thickness is given as input and the number of layers (n). Effective modulus (E) of the material is obtained from the experimental results. The angle (a) of fiber layers of the specimen is given for four different layers. The results from the execution of the mat lab program gives the shear modulus for the GFRP specimen. The shear modulus for four different specimens can be obtained from varying the angles and effective modulus in the program for different GFRP laminates.

Failure can occur in any of four different ways [36]:

- If DFAILT is zero failure occurs if the chang/chang failure criterion is satisfied in the tensile fiber mode [36].
- If DFAILT is greater than zero failure occurs if the tensile fiber strain is greater than DFAILT or less than DFAILC [36].
- If EFS is greater than zero, failure occurs if the effective strain is greater than EFS [36].
- If TFAIL is greater than zero failure occurs according to the element time step as described in the definition of TFAIL above [36].

When failure has occurred in all the composite layers (through-thickness integration points), the element is deleted [36].

Material properties

Material properties assigned based on test data in the fiber and matrix direction [42]

XT, DFAILT	YT, DFAILM
XC, DFAILC	YC, DFAILM
EA	EB

Tsai–Hill Failure Criterion for Unidirectional Fiber Composites

This theory is based on the distortion energy failure theory of Von-Mises' distortional energy yield criterion for isotropic materials as applied to anisotropic materials. Distortion energy is actually a part of the total strain energy in a body [42]. The strain energy in a body consists of two parts; one due to a change in volume and is called the dilation energy and the second is due to a change in shape and is called the distortion energy. [42]

$$\left[\frac{\sigma_1}{(\sigma_1^T)_{ult}}\right]^2 - \left[\frac{\sigma_1\sigma_2}{(\sigma_1^T)^2_{ult}}\right] + \left[\frac{\sigma_2}{(\sigma_2^T)_{ult}}\right]^2 + \left[\frac{\tau_{12}}{(\tau_{12})_{ult}}\right]^2 < 1. \quad (4.1)\ [42]$$

Tsai–Wu Failure Criterion for Unidirectional Fiber Composites

This failure theory is based on the total strain energy failure theory of Beltrami. Tsai-Wu9 applied the failure theory to a lamina in plane stress [42]. A lamina is considered to be failed if is violated. This failure theory is more general than the Tsai–Hill failure theory because it distinguishes between the compressive and tensile strengths of a lamina. [42]

$$H_1\sigma_1 + H_2\sigma_2 + H_6\tau_{12} + H_{11}\,\sigma_1^2 + H_{22}\,\sigma_2^2 + H_{66}\,\tau_{12}^2 + 2H_{12}\sigma_1\sigma_2 < 1 \quad (4.2)\ [42]$$

Chang and Chang Failure Criterion for Unidirectional Fiber Composites

The understanding of the Chang criterion is much more complicated than in the case of the Hashin criterion and requires a consideration of Chang's work, in general, starting with his early works on failure matrix criterion.[42]

Matrix Cracking

$$\left(\frac{\sigma_{22}}{Y_T}\right)^2 + T = 1 \quad (4.3)\ [42]$$

Fiber Matrix and/ or Fiber Damage

$$\left(\frac{\sigma_{11}}{X_T}\right)^2 + T = 1 \qquad (4.4)\ [42]$$

Hashin's Failure Criteria for Unidirectional Fiber Composites

These are interacting failure criteria where more than one stress components have been used to evaluate the different failure modes. These criteria were originally developed for unidirectional polymeric composites, and hence, applications to other type of laminates and non-polymeric composites have significant approximations [36]. Usually Hashin criteria are implemented within two dimensional classical lamination approach for point stress calculations with ply discounting as the material degradation model. Failure indices for Hashin criteria are related to fiber and matrix failures and involve four failure modes. The criteria are extended to three dimensional problems where the maximum stress criteria are used for transverse normal stress component. The various failure modes in the sandwich structure is shown in (Figure 4.9) [36].

The failure modes included in Hashin's criteria are as follows.

1. Tensile fiber failure for $\sigma_{11} \geq 0$

$$\left(\frac{\sigma_{11}}{X_T}\right)^2 + \frac{\sigma_{12}^2 + \sigma_{13}^2}{S_{12}^2} = \begin{cases} \geq 1 & \text{failure} \\ < 1 & \text{no failure} \end{cases} \qquad (4.5)\ [36]$$

2. Compressive fiber failure for $\sigma_{11} < 0$

$$\left(\frac{\sigma_{11}}{X_C}\right)^2 = \begin{cases} \geq 1 & \text{failure} \\ < 1 & \text{no failure} \end{cases} \qquad (4.6)\ [36]$$

3. Tensile matrix failure for $\sigma_{22} + \sigma_{33} > 0$

$$\frac{(\sigma_{22} + \sigma_{33})^2}{Y_T^2} + \frac{\sigma_{23}^2 - \sigma_{22}\sigma_{33}}{S_{23}^2} + \frac{\sigma_{12}^2 + \sigma_{13}^2}{S_{12}^2} = \begin{cases} \geq 1 & \text{failure} \\ < 1 & \text{no failure} \end{cases} \qquad (4.7)\ [36]$$

4. Compressive matrix failure for $\sigma_{22} + \sigma_{33} < 0$

$$\left[\left(\frac{Y_C}{2S_{23}}\right)^2 - 1\right]\left(\frac{\sigma_{22}+\sigma_{33}}{Y_C}\right) + \frac{(\sigma_{22}+\sigma_{33})^2}{4S_{23}^2} + \frac{\sigma_{23}^2 - \sigma_{22}\sigma_{33}}{S_{23}^2} + \frac{\sigma_{12}^2 + \sigma_{13}^2}{S_{12}^2} = \begin{cases} \geq 1 & \text{failure} \\ < 1 & \text{no failure} \end{cases} \quad (4.8)\ [36]$$

5. Interlaminar tensile failure for $\sigma_{33} > 0$

$$\left(\frac{\sigma_{33}}{Z_T}\right)^2 = \begin{cases} \geq 1 & \text{failure} \\ < 1 & \text{no failure} \end{cases} \quad (4.9)\ [36]$$

6. Interlaminar compression failure for $\sigma_{33} < 0$

$$\left(\frac{\sigma_{33}}{Z_C}\right)^2 = \begin{cases} \geq 1 & \text{failure} \\ < 1 & \text{no failure} \end{cases} \quad (4.10)\ [36]$$

where, σ_{ij} denote the stress components and the tensile and compressive allowable strengths for lamina are denoted by subscripts *T* and *C*, respectively. X_T, Y_T, Z_T denotes the allowable tensile strengths in three respective material directions [36]. Similarly, X_C, Y_C, Z_C denotes the allowable compressive strengths in three respective material directions. Further, S_{12}, S_{13} and S_{23} denote allowable shear strengths in the respective principal material directions [36].

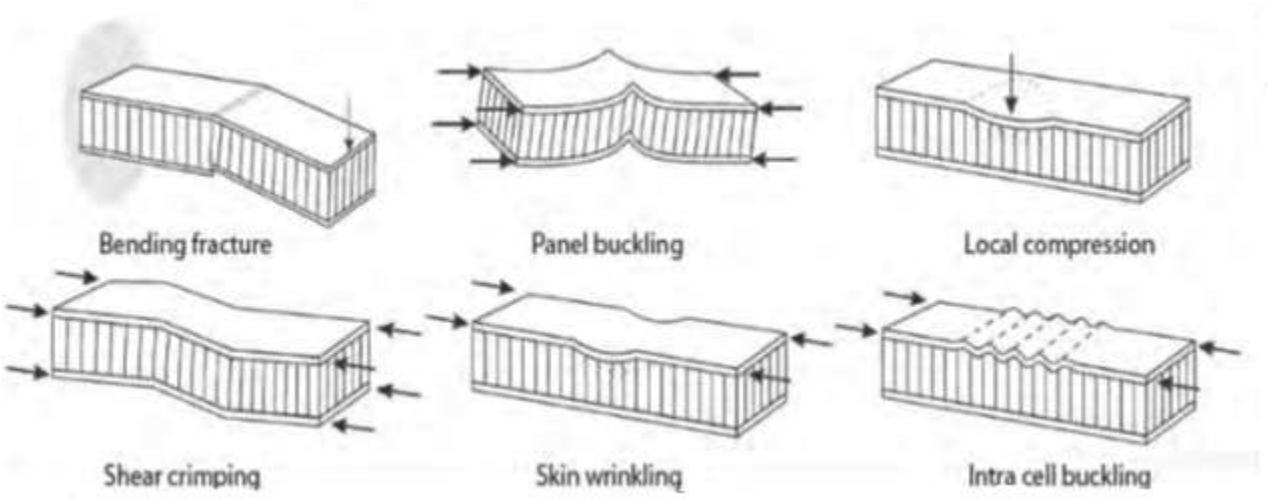

Figure 4.9: Failure modes for sandwich structure [36]

4.2.4 Effective Young's Modulus by Analytical Approach

The formulas used in matlab for the calculation of material properties,

The definition of Poisson ratio

$$v_{21} = \frac{E_2 \cdot v_{12}}{E_1} \tag{4.12}$$

The in-plane shear modulus of the fiber

$$G_{12} = \frac{E_2}{(2*(1+V_{21}))} \tag{4.13}$$

$$S = \begin{bmatrix} S_{11} & S_{22} & S_{26} \\ S_{21} & S_{22} & S_{26} \\ S_{61} & S_{62} & S_{66} \end{bmatrix}$$

$$A = \left(\frac{t_1}{t*A1} + \frac{t_2}{t*A2} + \frac{t_3}{t*A3} + \frac{t_4}{t*A4}\right) \tag{4.14}$$

The shear modulus of the fiber

$$S_{ef} = \frac{1}{A^{-1}} \tag{4.15}$$

Where v_{12}, v_{21} are the Poisson ratio. The longitudinal and transverse Young's modulus of the laminate is denoted by E_1, E_2. The effective Young's modulus were obtained from the results of the analytical method calculations. The in-plane shear modulus of the fiber is given by G_{12}. The thickness of the laminate in each layer is denoted by t_1, t_2, t_3, t_4. A_1, A_2, A_3, A_4 is the area of the fiber in four different laminate layers and A is the total area of the laminate. The S_{ef} is the shear modulus of the laminate.

4.2.5 Analytical Results of Tension Test of GFRP with Differently Oriented Layers

The results from the analytical mat lab calculations is given in the (Table 4.5). The results for four different angles of specimens 0^o, 30^o, 60^o, 90^o is compared with the simulation and experimental results.

Table 4.5: Results obtained from analytical method for GFRP laminates

Result for 0 Degree	**Result for 30 Degree**
S_{ef} = 27.8000 -99.2857 Inf -99.2857 8.0800 Inf Inf Inf 3.7360	S_{ef} = 18.4908 -34.5365 -Inf -34.5365 8.4285 -Inf Inf Inf 6.6117
Result for 60 Degree	**Result for 90 Degree**
S_{ef} = 8.6608 -30.2477 -Inf -30.2477 16.6422 -Inf Inf Inf 7.0770	S_{ef} = 8.0800 -99.2857 Inf -99.2857 27.8000 Inf Inf Inf 3.7360

4.2.6 Experimental vs Analytical vs Simulation Graphs

The tensile behavior of the composite facesheet is shown in (Figure 4.10, 4.11, 4.12, 4.13) for four different angles. According to this figure, the obtained simulation, analytical and experimental results were in good correlation with each other.

0 Degree

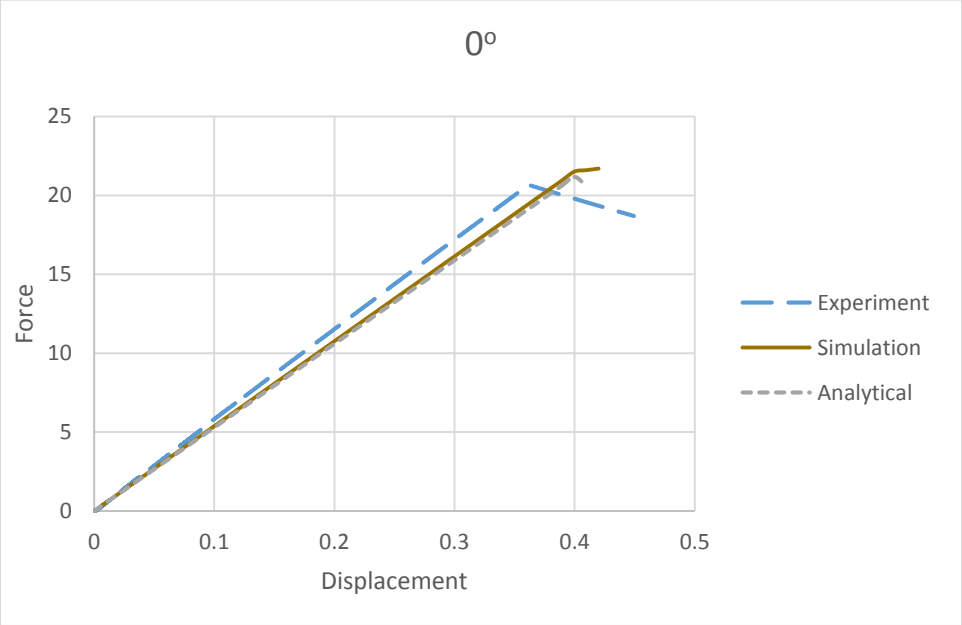

Figure 4.10: Graph for 0 Degree GFRP laminates

30 Degree

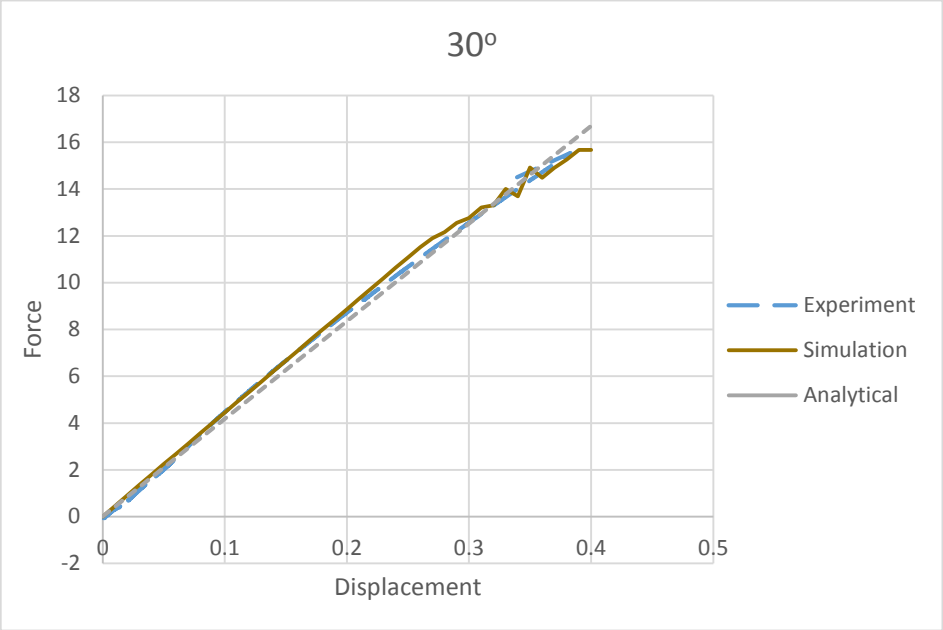

Figure 4.11: Graph for 30 Degree GFRP laminates

60 Degree

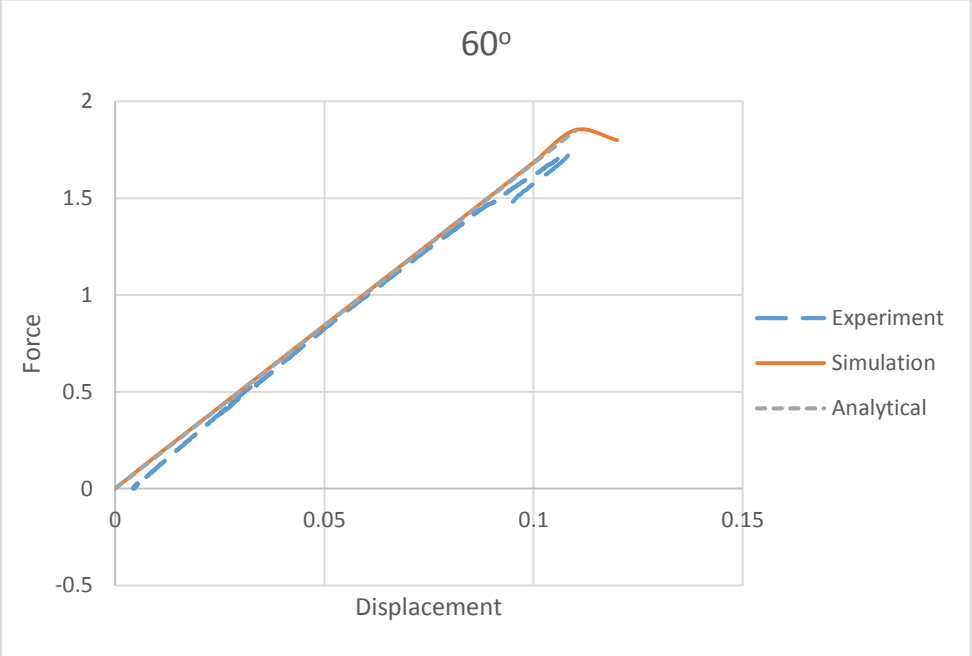

Figure 4.12: Graph for 60 Degree GFRP laminates

90 Degree

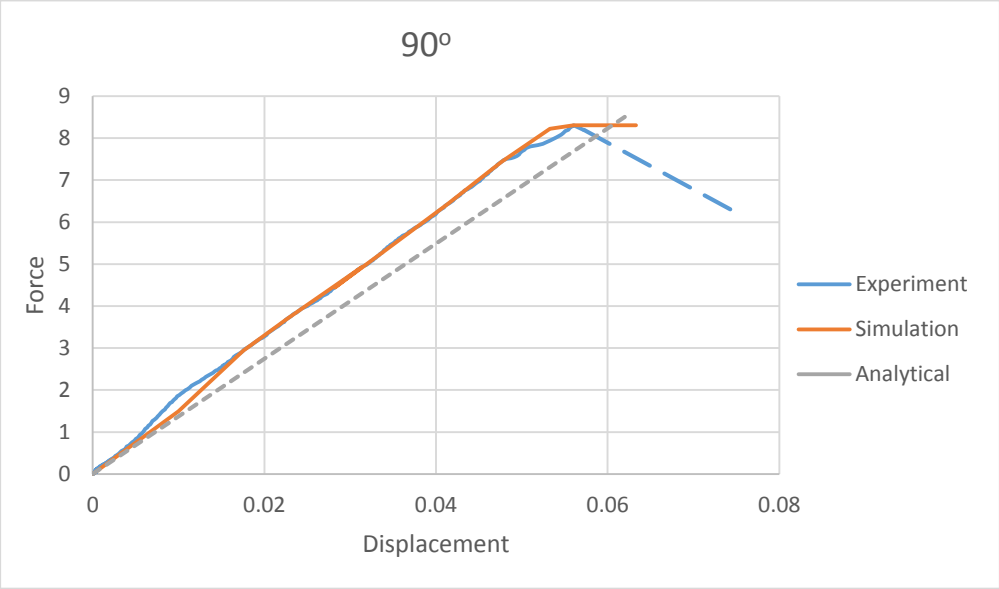

Figure 4.13: Graph for 90 Degree GFRP laminates

4.3 Three Point Bending Test on GFRP Sandwich Structure

The dimensions of the bending test specimens were as follows: width 60 mm, the thickness of top facesheet 3.0 mm, the thickness of bottom facesheet 2.4 mm, the core thickness 10 mm, the sandwich thickness 15.4 mm ($[\pm 65^o]_2$ /core/ $[\pm 65^o/90^o]$) and the distance between supports 200 mm [37]. The force versus the deflection was measured during this test (Figure 4.18). At a deflection of 2.6 mm, the effective failure strain of honeycomb core material has reached the limit value in the middle of the sandwich. Decreasing of force begins at this point (Figure 4.17).

The blue areas (Figure 4.17) show the locations and size of failed zones in the glue layer and core. Before the maximum bending force is reached (at the deflection of 2.5 mm) the significant failure area of the glue layer can be seen and no failures are observed in the core material [37]. As the deflection increases up to 3.0 mm, the debonding area remains constant but failure of the core occurs. The decrease of the bending force coincides with beginning of the core failure [37]. Fitted material constants (Table 3.1) which gives a good coincidence between experimental and simulation results were used for the further simulations.

4.3.1 Experimental Results

Table 4.6: Results obtained from experimental calculations of GFRP sandwich structure

No	Orientation	b mm	h mm	Core Height t mm	t_i mm	t_e mm	Force kN	Deflection mm	L_0 mm
L1	Longitudinal Direction	29.5	17.0	9.6	3.4	4.0	0.576	3.618	200
L2		30.0	17.2	9.8	3.4	4.0	0.588	3.190	200
L3		31.0	17.5	10.1	3.4	4.0	0.540	2.861	200
L4		47.0	22.0	14.6	3.2	4.2	0.780	3.914	200
R1	Circumferential Direction	30.0	17.0	9.6	3.4	4.0	1.614	4.049	200
R2		31.4	17.0	9.6	3.4	4.0	1.710	2.879	200
R3		30.5	17.0	9.6	3.4	4.0	1.554	3.100	200
R4		32.0	17.0	9.6	3.4	4.0	1.824	2.993	200
R5		50.0	22.0	14.6	3.2	4.2	2.088	6.225	200

4.3.2 Finite Element Method

4.3.2.1 Ls – Dyna

The composite sandwich structure was modeled with facesheets mad of glass fiber facesheets and a paper honeycomb core has been modelled with (*Part_Composite) [37]. The bonding between the honeycomb core and facesheets has been modelled by embedding glue layers. The dimensions of the sandwich structure are: width 60 mm, the thickness of top facesheet 3.0 mm, the thickness of bottom facesheet 2.4 mm, the core thickness 10 mm, the sandwich thickness 15.4 mm ($[\pm 65^o]_2$ /core/ $[\pm 65^o/90^o]$) and the distance between supports 200 mm [37].

The (Figure 4.14) denotes a composite sandwich structure is subjected to three point bending test. The bottom part of the composite is supported by two fixed ends and at the middle of the composite the load is applied at a constant rate of 100 mm/s. The (Figure 4.15) represents the von misses stress acting on

the GFRP composite. The red zone in the figure denotes the weak zones in the GFRP composite and the crack of the composite starts from this zone. The crack continues to grow and breakage finally occurs in the GFRP composite.

Figure 4.14: Sandwich composite with fixed and load applied nodes

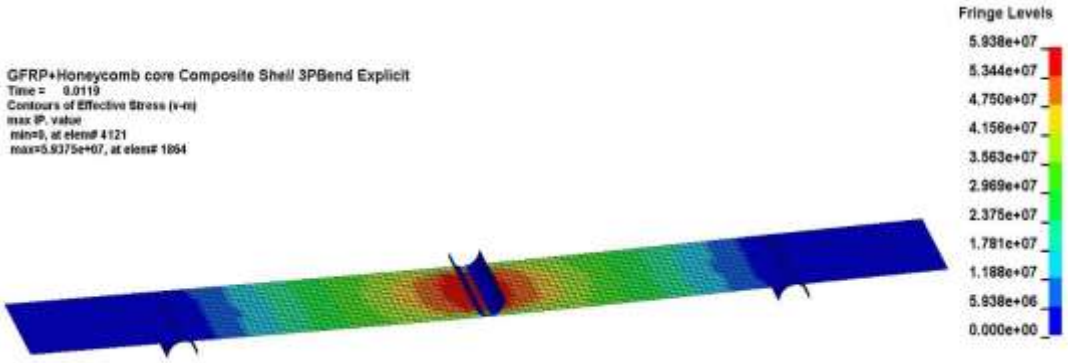

Figure 4.15: Von misses stress acting in GFRP composite

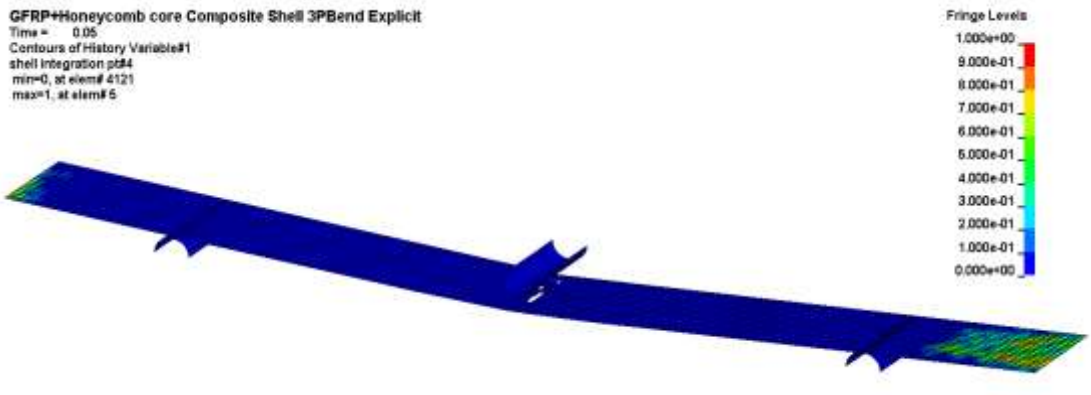

Figure 4.16: The Breakage point in GFRP composite beam

The (Figure 4.16) shows the breakage point in GFRP composite and the red zones shows the point at which the maximum stress is acting on the laminate.

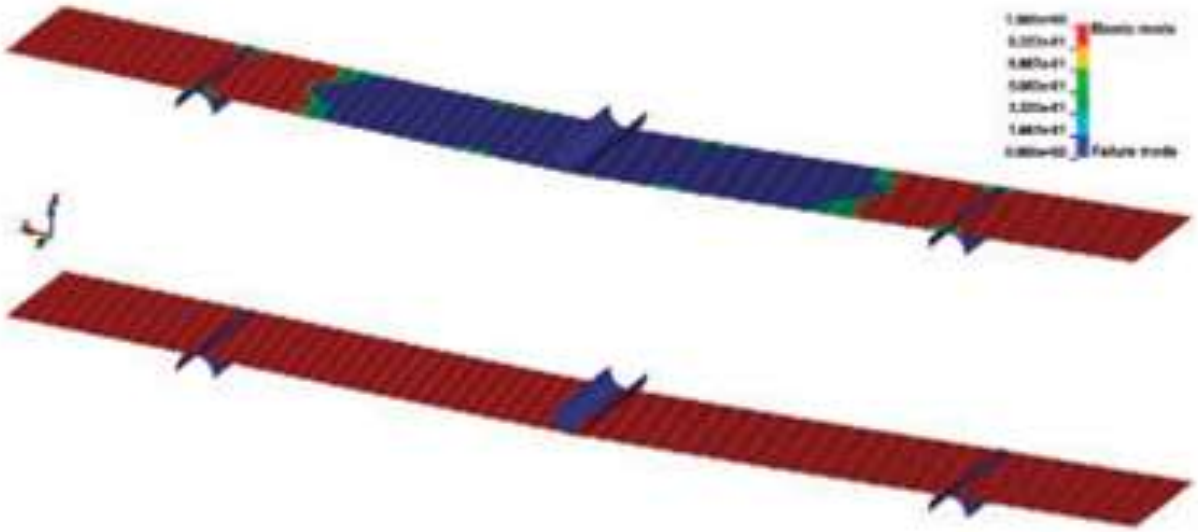

Figure 4.17: Three-point bending test of sandwich structure failure modes in glue and core layers at different deflections

4.3.3 Experimental vs Finite Element Graphs

The experimental and the finite element results for the three point is shown in (Figure 4.18). During the first part of the curve the experimental and the finite element results were matching with each other.

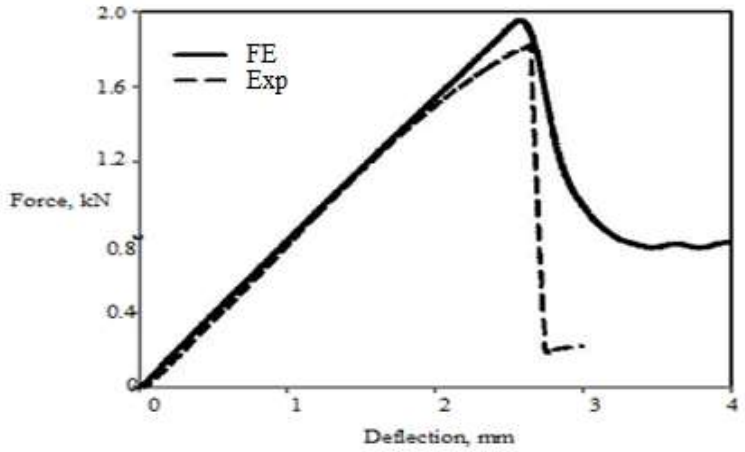

Figure 4.18: Three-point bending test of sandwich structure force versus deflection curves obtained experimentally and by FE simulation [37]

4.4 Compression Test on GFRP Cylinder Ring

The finite element model has a hollow cylinder of internal diameter D_c = 600 mm and width b_c = 196 mm is designed. The wall of the cylinder was defined as sandwich GFRP composite with a honeycomb core. The facesheet inside the cylinder had three layers; the laminate code was [±65°/90°] [37]. The external facesheet had four layers; the laminate code was $[\pm 65^o]_2$ [37]. The layers of angle of ply equal to 90° and ±65° had thicknesses 0.9 mm and 0.75 mm, respectively. The total thickness of the internal facesheet was equal to 2.4 mm; the external facesheet thickness was of 3.0 mm. The thickness of the core was equal to 10 mm [37].

The rings were loaded until failure occurred and the force decrease was observed. The first stage of the compression loading, it has been seen that cell walls distorted linearly. The Core cell walls distorted due to the local buckling, which limited the ultimate strength, and a relatively sudden collapse took place after the maximum load levels [37].. The curves it can be seen that the core materials experience the maximum force levels at lower deformation values. In both the numerical and experimental investigations, the same compression loading conditions were used. The verification of the model is presented in (Figure 4.20).The separated zones of tested samples were matching with the FE simulation results, which are presented in (Figure 4.20) [37].

The composite cylinder ring with fixed and load applied nodes is shown in (Figure 4.19).

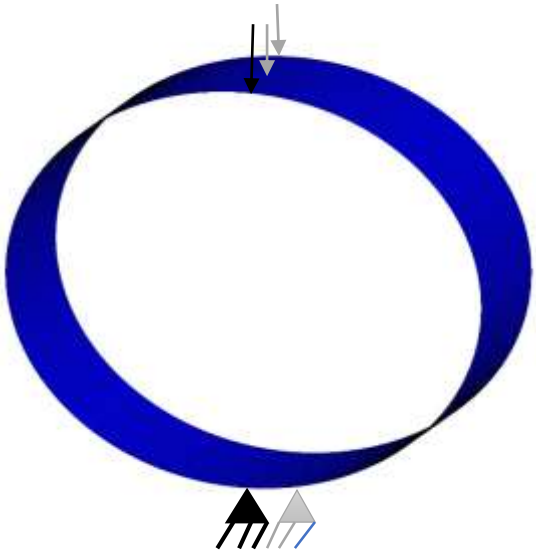

Figure 4.19: Composite cylinder ring with fixed and load applied nodes

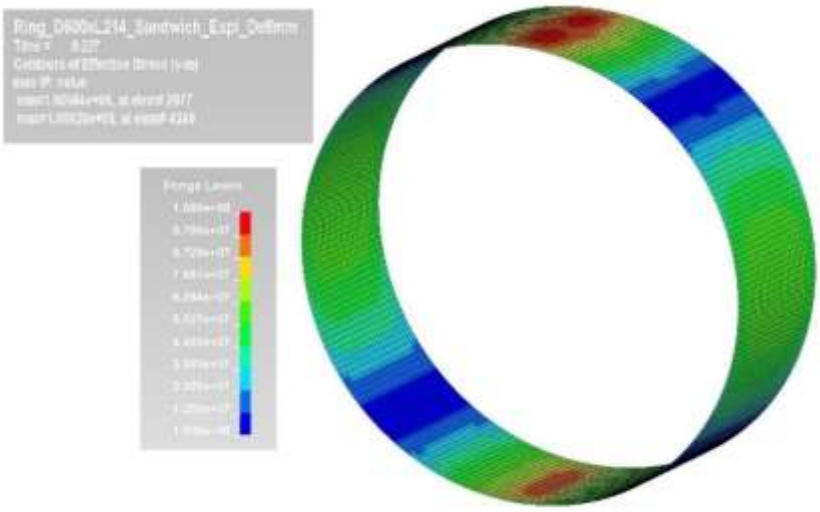

Figure 4.20: Verification of cylinder FE model: Damaged areas in core layer

4.4.1 Experimental vs Finite Element Graphs

The below figure shows the experimental results and finite element result for the ring compression test is given in (Figure 4.21).

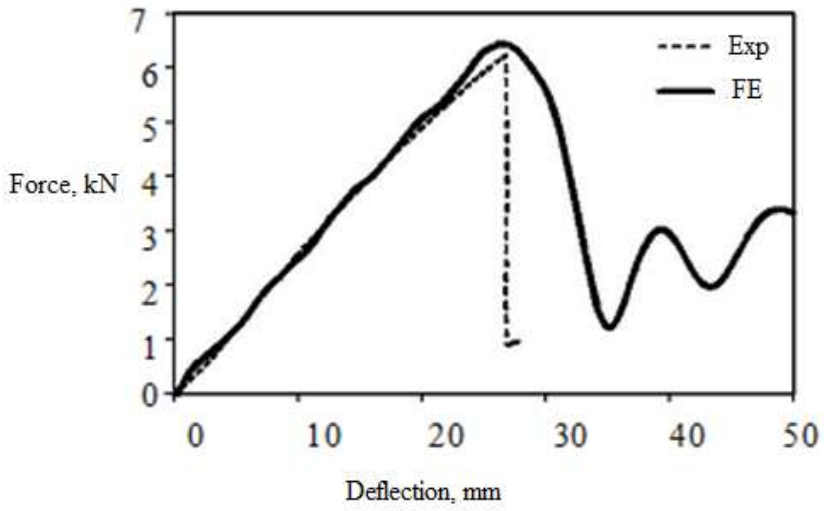

Figure 4.21: Verification of cylinder FE model: experimental and numerical results [37]

The (Figure 4.21) shows the graph for the ring compression test and the results were coinciding with each other for the experimental and the finite element results.

CONCLUSION

The stress analysis on the composite sandwich structures with recycled paper based honeycomb core and glass fiber reinforced polymer facesheets fabricated by filament winding process has been completed.

This methodology can be applied for all types of composite sandwich structures to determine the strength of the structures. The results from the analysis of the composite sandwich structures has been described below,

1. The materials of the separate components of sandwich structures were tested and their mechanical properties were determined. The Young's modulus of the facesheets from the experiment is 27.8 GPa. The stiffness of the specimen is obtained from the three point bending test. The individual performance of the paper honeycomb core material and E-glass fiber facesheets was also determined by performing tests on the materials.
2. The experimental result is taken as the base for the calculation and then it is compared with the analytical results. The analytical method on facesheet describes the Young's modulus value of the material difference with the experimental results by 2%.
3. The sandwich structure can be checked by finite element analysis technique to conduct three different tests were performed. The tension test, three point bending test and compression test were conducted on the composite specimens. The tension test allowed the verification of the material model and the failure criteria of the GFRP. The three point bending test and the ring compression test allowed the verification of the sandwich structure models.
4. The Finite element results from the tension, three point bending and compression tests models were designed and validated. The results of the tension test on the facesheet specimen was tested and it had been seen that the compressive modulus and strength values are higher in ply lay-up direction than in-plane direction. The three point bending test results showed that at first the de-bonding failure between the facesheets and the core occurred and after that the failure of the core appeared.
5. During the ring compression test same failure modes as in the three-point bending test were seen. The core failure followed after debonding. The shear stress in the glue layer started the debonding. The stiffness in the structure is decreased by the damages in the core. It has been observed that the core material influences the compressive properties of sandwich panel. The results from the

experimental tests is compared with finite element results. The comparison of the results shows a deviation of results by 6% between finite element and experimental results.

REFERENCES

1. Smallman, R.E., and R.J. Bishop. Modern Physical Metallurgy and Materials Engineering. 6th ed. Oxford: Butterworth-Heinemann, 1999.
2. Accelerating utilization of new materials, National Research Council (U.S.) Committee on Accelerated Utilization of New Materials, Washington, National Academy of Sciences – National Academy of Engineering, Springfield, Va, 1971, pages 56–57 by W P Conrardy.
3. Synthetic Resin – Use in Aircraft Construction, The Times, London England, Monday 5 October 1936, page 14, Issue 47497.
4. Reinforced plastics handbook; Donald V. Rosato, Dominick V. Rosato, and John Murphy; Elsevier; 2004; page 586.
5. Traidenis brochures on products of the Tanks.
6. Mayer, Rayner M. (1993), Design with reinforced plastics, Springer, p. 7, ISBN 978-0-85072-294-9.
7. Forbes Aird (1 April 1996). Fiberglass & Composite Materials: An Enthusiast's Guide to High Performance Non-Metallic Materials for Automotive Racing and Marine Use. Penguin. pp. 86– . ISBN 978-1-55788-239-4. Retrieved 12 June 2012.
8. Reinforced Plastics - World's largest FRP acid storage tanks. ScienceDirect.com. 2005-11-18. Retrieved 2013-04-22.
9. Kaw A.K. Mechanics of Composite Materials second Edition (Mechanical and Aerospace Engineering Series) CRC Press, Publication Date: November 2, 2005, ISBN-10: 0849313430, ISBN-13: 978-0849313431, Edition: 2.
10. Wahl, L.; Maas, S.; Waldmann, D.; Zurbes, A.; Freres, P. (28 May 2012)."Shear stresses in honeycomb sandwich plates: Analytical solution, finite element method and experimental verification". Journal of Sandwich Structures and Materials 14 (4): 449–468.
11. Bitzer, T (1997). Honeycomb Technology: Materials, Design, Manufacturing, Applications and Testing, London: Chapman & Hall.
12. Containment solutions brochures on products of the Tanks.
13. Composite Materials Ed. By L.J. Broutmen and R.H. Krock, Academic press, Volume 1-8, 1973 – 1976.

14. Cutler, John Henry; Koppel, Ivan; Liber, Jeremy. Understanding Aircraft Structures. Blackwell Publishing Limited. p. 14. ISBN 1-4051-2032-0.
15. Gere, James M (2004). Mechanics of Materials. Thomson Brooks/Cole. pp. 393–463. ISBN 0-534-41793-0.
16. R. Satheesh Raja , K. Manisekar , V. Manikandan Materials and Design "Study on mechanical properties of fly ash impregnated glass fiber reinforced polymer composites using mixture design analysis" Department of Mechanical Engineering, PET Engineering College, India.
17. A Akdemir, N Tarakcioglu, , A Avci "Stress corrosion crack growth in glass/polyester composites with surface crack" Department of Mechanical Engineering, Engineering Faculty, Muh-Mim Faculty Kampus, Selcuk University, Konya, Turkey.
18. Karl Hoffmann (1987) An Introduction to Measurements using Strain Gauges Publisher: Hottinger Baldwin Messtechnik GmbH, Darmstadt.
19. R.Balasubramaniam Callisters "Material Science and Engineering" Wiley India (P) Ltd ISBN: 978-81-265-2143-2. Pages 539-570.
20. R. Gardon, in: D.R. Uhlmann, N.J. Kreidl (Eds.), Glass: Science and Technology, Elasticity and Strength in Glasses, vol. 5, Academic Press, New York, 1980, pp. 146–216.
21. http://en.wikipedia.org/wiki/Fibre-reinforced_plastic
22. M. Tomozawa, P.J. Lezzi, R.W. Hepburn, T.A. Blanchet, D.J. Cherniak, J. Non-Cryst. "Solids Surface stress relaxation and resulting residual stress in glass fibers: A new mechanical strengthening mechanism of glasses" Department of Mechanical, Aerospace and Nuclear Engineering, Rensselaer Polytechnic Institute, Troy, NY 12180-3590, USA, 6 July 2012.
23. P.J. Lezzi , Q.R. Xiao, M. Tomozawa, T.A. Blanchet, C.R. Kurkjian "Strength increase of silica glass fibers by surface stress relaxation: A new mechanical strengthening method" Department of Materials Science and Engineering, Rensselaer Polytechnic Institute, Troy, NY 12180-3590, USA, 26 August 2013.
24. Hong Li, Cheryl Richards and James Watson, "High-Performance Glass Fiber Development for Composite Applications" Volume 5, Issue 1, pages 65–81, March 2014
25. https://www.coursehero.com/tutors-problems/Mechanical-Engineering/7744308-You-are-asked-to-produce-an-aligned-and-continuous-fiber-reinforced-ep/ Abeyshinge HP, Ghotra JS, Pritchard G. "Substances contributing to the generation of osmotic pressure in resins and laminates". Composites 1983; 14:57–61.

26. Abeyshinge HP, Ghotra JS, Pritchard G. “Substances contributing to the generation of osmotic pressure in resins and laminates”. Composites 1983; 14:57–61.
27. Kellas S, Morton J, Curtis PT. “The effect of hygrothermal environments upon the tensile and compressive strengths on notched CFRP laminates. Part I: Static loading”.Composites 1990;21:41–51.
28. http://encyclopedia2.thefreedictionary.com/Displacement+Transducer.
29. Crowther MF, Wyatt RC, Phillips MG. “Creep-fatigue interactions in glass fibre/polyester composites”. Composites Science and Technology 1989; 36:191–210.
30. Felippa, Carlos A. 2004. Introduction to the Finite Element Method. University of Colorado, Colorado. http://www.colorado.edu/ (accessed October 15, 2014).
31. Chen Y. 2000, Finite Element Micromechanical Modeling of Glass Fibedepoxy Crossply Laminates. University of Alberta Thesis of MS.
32. Okutan, B. 2001. Stress and failure analysis of laminated composite pinned joints. Dokuz Eylül University Thesis of PhD.
33. Chen Y. 2000, Finite Element Micromechanical Modeling of Glass Fibedepoxy Crossply Laminates. University of Alberta Thesis of MS.
34. Chou, Tsu-Wei. 1991. Microstructural design of fiber composites. Cambridge: Cambridge University Press.
35. Chang FK and Chang KY. Post-failure analysis of bolted composite joints in tension or shear-out mode failure. J Compos Mater 1987; 21: 809–833.
36. Hashin Z. Failure criteria for unidirectional fiber composites. J Appl Mech 1980; 47: 329–334.
37. Daiva Zeleniakiene, Vitalis Leisis and Paulius Griskevicius. “A numerical study to analyse the strength and stiffness of hollow cylindrical structures comprising sandwich fiber reinforced plastic composites”. Journal of Composite Materials. Downloaded from jcm.sagepub.com at Kaunas University of Technology on January 13, 2015.
38. Hallquist JO. LS-DYNA Theoretical manual. Livermore Software Technology Corporation, March 2006.
39. Heimbs S, Middendorf P, Maier M, et al. Honeycomb sandwich material modeling for dynamic simulations of aircraft interior components. In: 9th International LSDYNA users conference. Dearborn: USA, 4–6 June 2006, p.20-1-20-14.

40. B. Elliott and N. Petrinic. “Strategies for effciency in inverse modelling of material parameters for predictive modelling of aerospace alloys”. Compututional Fluid and Solid Mechanics. Elsevier LTd., 2005.
41. Sami A. Alsh'urafa “Theoretical Study on the Effects of Various Vf on the Flexural Strength and Stiffness of non-Pre-stressed FRP Plates Reinforced Timber Beams” International Journal of Engineering, Business and Enterprise Applications (IJEBEA) Engineering Management Department Prince Sultan University ISSN : 2279-0039.
42. Federico Paris “A Study of Failure Criteria of Fibrous Composite Materials” George Washington University, Joint Institute for the Advancement of Flight Sciences Langley Research Center, Hampton, Virginia

APPENDIX A Mat Lab Program for Tension Test on Laminate

The following source code was used to implement the model proposed in Chapter 4 and calculate the stress, strain for an LS DYNA/Standard user defined material.

```
clc

t=3.6; n=4; t_1=t/4; t_2=t/4; t_3=t/4; t_4=t/4;

E_1=27.8; E_2=8.08; v_12=0.28;

v_21=E_2*v_12/E_1

G_12=E_2/(2*(1+v_21))

a_1=0; a_2=0; a_3=0; a_4=0;

c1=cosd(a_1); c2=cosd(a_2); c3=cosd(a_3); c4=cosd(a_4);

s1=sind(a_1); s2=sind(a_2); s3=sind(a_3); s4=sind(a_4);

S_11=1/E_1; S_12=-v_12/E_1; S_21=S_12; S_22=1/E_2;

S_16=0; S_26=S_16; S_61=S_16; S_62=S_16; S_66=1/G_12;

S=[S_11 S_12 S_16; S_21 S_22 S_26; S_61 S_62 S_66]

Q=S^-1;

R=[1 0 0; 0 1 0; 0 0 2];

T1=[c1^2 s1^2 2*s1*c1; s1^2 c1^2 -2*s1*c1; -s1*c1 s1*c1 c1^2-s1^2];

T2=[c2^2 s2^2 2*s2*c2; s2^2 c2^2 -2*s2*c2; -s2*c2 s2*c2 c2^2-s2^2];

T3=[c3^2 s3^2 2*s3*c3; s3^2 c3^2 -2*s3*c3; -s3*c3 s3*c3 c3^2-s3^2];

T4=[c4^2 s4^2 2*s4*c3; s4^2 c4^2 -2*s4*c4; -s4*c4 s4*c4 c4^2-s4^2];

A1=T1^-1*Q*R*T1*R^-1;  A2=T2^-1*Q*R*T2*R^-1;  A3=T3^-1*Q*R*T3*R^-1;  A4=T4^-
1*Q*R*T4*R^-1;
```

A=(t_1/t*A1+t_2/t*A2+t_3/t*A3+t_4/t*A4)

a=A^-1

S_ef=1./A^-1

v_xy=-a(1,2)/a(1,1)

v_yx=-a(1,2)/a(2,2)

APPENDIX B LS DYNA/Standard Material Cards

The following LS DYNA/Standard elastic laminate material control cards, with various field dependencies, were calibrated from experimental test data.

```
$# LS-DYNA Keyword file created by LS-PrePost 4.2 (Beta) - 31Oct2014(14:00)
$# Created on Sep-07-2015 (23:32:59)
*KEYWORD MEMORY=240M
*TITLE
$#
*MAT_ENHANCED_COMPOSITE_DAMAGE
$#  mid        ro        ea        eb        (ec)      prba     (prca) (prcb)
       1 1800.00001.7700E+10 4.0000E+9 4.0000E+9 8.0000E-2 8.0000E-2 8.0000E-2
$#     gab       gbc       gca        (kf)      aopt
 7.4000E+9 1.8500E+9 7.4000E+9       0.000  2.000000

$#      xp        yp        zp        a1        a2        a3    mangle
     0.000     0.000     0.000  1.000000     0.000     0.000     0.000
$#      v1        v2        v3        d1        d2        d3   dfailm   dfails
     0.000     0.000     0.000     0.000     0.000     0.000 2.0000E-2 2.0000E-2
$#   tfail      alph      soft      fbrt     ycfac     dfailt    dfailc    efs
     0.000     0.000     0.000     0.000     0.000 4.0000E-2 -2.000E-2  0.000
$#      xc        xt        yc        yt        sc      crit      beta
 2.0000E+8 6.4400E+8 2.0000E+8 1.9600E+7 2.1400E+7 54.000000     0.000
$#     pel      epsf      epsr      tsmd     soft2
     0.000     0.000     0.000     0.000  1.000000
$#  slimt1    slimc1    slimt2    slimc2     slims    ncyred     softg
     0.000     0.000     0.000     0.000     0.000     0.000  1.000000
```

Material Properties: Elastic

Material Properties: Strength and Strain to Failure